



REVIEW

Advances in nonlinear acoustic/elastic metamaterials and metastructures

Xin Fang · Walter Lacarbonara · Li Cheng

Received: 2 May 2024 / Accepted: 22 August 2024 / Published online: 3 September 2024
© The Author(s) 2024

Abstract Acoustic/elastic metamaterials exhibit a wealth of unusual properties conducive to wave manipulation. This review outlines state-of-the-art developments from FPUT chains, granular crystals to nonlinear acoustic metamaterials (NAMs). It mainly discusses key advances made in the domain of NAMs for wave manipulation, vibration control and sound attenuation given the blooming interest in exploring how nonlinearity offers possibilities for discovering novel wave phenomena, principles and properties that potentially go well beyond linear metamaterials and the relevant linear theories. NAMs reveal intriguing wave phenomena, revolutionizing our understanding of wave behavior including the breakdown of reciprocity, stationary invariance and space–time invariance, and have the potential to promote superior engineering

performance like ultra-low and ultra-broadband vibration reduction. An overview of present research and further challenges are provided in fields such as calculation methods, amplitude-dependent bandgaps, self-adaptive bands, nonreciprocal wave control, harmonic control, chaotic dynamics, vibration and sound attenuation, practical design, experimental implementation, and practical applications.

Keywords Nonlinear acoustic metamaterials · Nonlinear elastic metastructures · Nonlinear dynamics · Nonlinear wave control · Review · Advances

X. Fang (✉)
National Key Laboratory of Equipment State Sensing and Smart Support, College of Intelligent Science, National University of Defense Technology, Changsha 410073, Hunan, China
e-mail: xinfangdr@sina.com

W. Lacarbonara
Department of Geotechnical and Structural Engineering, Sapienza University of Rome, Rome, Italy
e-mail: walter.lacarbonara@uniroma1.it

L. Cheng
Department of Mechanical Engineering, Hong Kong Polytechnic University, Hong Kong, China
e-mail: li.cheng@polyu.edu.hk

1 Introduction

Since the early investigations into the three-body problem, a deeper understanding of nonlinear dynamics of low-dimensional systems has been achieved over the last century. In 1955, the enigmatic Fermi-Pasta-Ulam-Tsingou (FPUT) paradox emerged, challenging conventional understanding about wave propagation in nonlinear periodic systems [1, 2]. In the following seven decades, extensive studies into the FPUT paradox have catalyzed a significant shift in nonlinear science and physics [3]. Remarkably, investigations into nonlinear phononic crystals (NPCs) [4], especially granular crystals [5], which serve as prime examples of nonlinear periodic

systems, have unveiled a wealth of intriguing wave properties over the last three decades [6–8]. An overview of the overarching progress of these advances is depicted in Fig. 1.

Metamaterials, often characterized by their unusual subwavelength properties and periodic structure, have been the subject of intense research for over two decades [9–11]. Studies have unveiled fascinating wave phenomena and ushered in potential applications in various domains, including vibration and noise control, wave energy harnessing, and acoustic/elastic wave sensing [12–14]. However, most of the existing research has been focused on linear metamaterials (LAMs), rooted firmly in the theories of linear elasticity based on several fundamental assumptions, such as small deformations, mono-frequency harmonic responses, the preservation of frequency, reciprocal propagation, space–time invariance, etc. This linear perspective has hindered the exploration of new opportunities stemming from intricate nonlinear dynamic behaviors. Moreover, sound and vibration control methods centered on locally resonant bandgaps in LAMs frequently encounter a narrow bandwidth, relying heavily on the attached mass ratio. Therefore, progressing from linear to nonlinear studies not only aligns with the scientific evolution from linear to nonlinear dynamics, but more importantly, unlocks a new realm of possibilities for discovering novel wave phenomena, establishing new principles, overcoming limitations imposed by linear theories, and addressing a wider array of engineering needs. For example, studies on nonlinear electromagnetic metamaterials [15–18] have revolutionized our understanding of the nonlinear world, enriching the body of knowledge in nonlinear physics and dynamics, and

paving the way towards groundbreaking applications [19].

Since approximately 2016, nonlinear acoustic metamaterials (NAMs) [20–24], with embedded nonlinear local resonators, have garnered growing interest. Existing findings have established the foundation for exploring, designing, and utilizing nonlinear metamaterials. Studies revealed unique properties absent in their linear counterparts. These distinctive characteristics include, among others, amplitude-dependent bandgaps [25], sub-harmonic bandgaps [26], self-adaptive band and actions [27], chaotic bands [22], higher-order harmonics [28], non-reciprocity [29, 30]. Recent investigations demonstrated that nonlinearities within meta-structures can produce remarkable vibro-acoustic effects, such as ultra-low and ultra-broadband vibration suppression [23] associated with nonlinear local resonances, and the can overcome the conventional law mass limitations in acoustic insulation [31].

Therefore, the integration of nonlinearity into acoustic metamaterials offers exciting opportunities for the creation of novel devices and systems with new wave manipulation capabilities [20–23]. However, the complexity and unique features of these systems demand a concerted effort from the scientific community to develop new theoretical paradigms, simulation techniques, and experimental methods to fully unlock their potential, although substantial progress is continuously being made. Currently, there is a surge of interest in nonlinear metamaterials, in view of their potential to induce abundant unusual behaviors including novel wave dynamics, thereby pushing the boundaries of nonlinear dynamics.

This paper aims to provide a comprehensive and timely overview of the advances on nonlinear

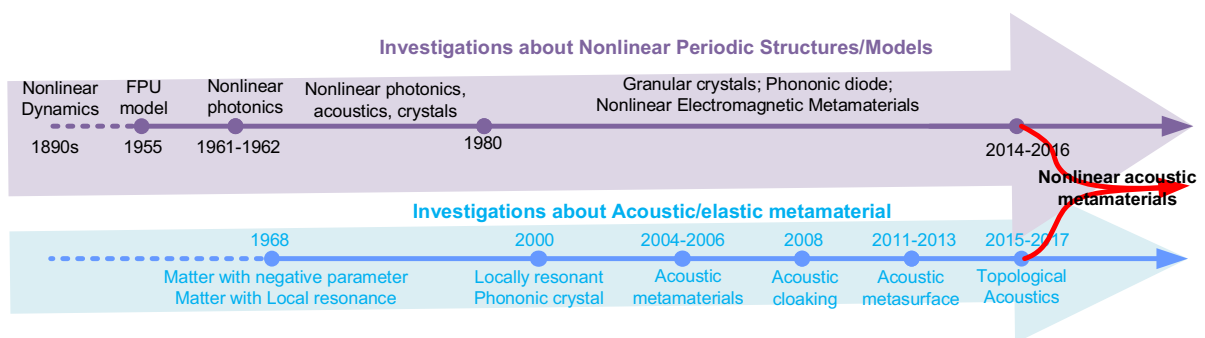


Fig. 1 Development routes of “nonlinear periodic structure/system” and “acoustic/elastic metamaterials”

acoustic/elastic metamaterials (NAMs). First, we outline the development trajectory of NAMs starting from wave manipulation in linear metamaterials, nonlinear crystals and nonlinear periodic structures (Sect. 2). Secondly, we elaborate important phenomena and effects of nonlinear wave dynamics enabled by NAMs, paying more attention to physical mechanisms (Sect. 3). Thirdly, we analyze the vibration and sound attenuation of NAMs in applications (Sect. 4). While summarizing the advances in several directions, we also discuss the challenges and possibilities of further developments of NAMs. While trying to be broad and deep in reviewing nonlinear wave dynamics, we strive to keep the review as succinct and accessible as possible.

2 From linear to nonlinear acoustic metamaterials

The emerging technology of meta-materials/structures offers an exciting route to achieve unprecedented wave control capabilities. Over the past two decades, a rich array of linear acoustic metamaterials (LAMs) has been investigated within the framework of linear dynamics.

2.1 Linear acoustic metamaterials

As early as the 1960s, scientists discovered that when impurities (or defects) exist in an ideal crystal (such as silver impurities in potassium chloride crystals), local resonances can be generated near the impurities (or defects) [32, 33], inducing low-frequency wave absorption. At the end of twentieth century, bandgaps in linear phononic crystals were extensively studied [34, 35]. In 2000, Liu et al. embedded locally resonant microstructures into an elastic matrix to create a locally resonant phononic crystal [9, 36], offering significant wave attenuation at deeply subwavelength scale. Locally resonant metamaterials induce negative effective mass density, negative effective modulus [37] and low-frequency bandgaps for blocking wave propagation. Their behavior can still be cast into Hooke's law (σ - ε) and Newton's second law between force F and acceleration a : $\sigma = E_{\text{eff}}\varepsilon$, $F = m_{\text{eff}}a$, where E_{eff} and m_{eff} denote the effective dynamic modulus and mass of the metamaterial, respectively. For example, for a linear diatomic meta-cell (see Fig. 2a), one has

$$m_{\text{eff}} = \frac{\langle F \rangle}{\langle a \rangle} = m_0 + \frac{k_r}{\omega_r^2 - \omega^2} \quad (1)$$

where m_0 denotes the primary mass; k_r and ω_r denote the stiffness and frequency of local resonators, respectively. It turns out that $m_{\text{eff}} < 0$ for $\omega_r < \omega < \sqrt{\omega_r^2 + k_r/m_0}$. An array of Helmholtz resonators can realize effective negative modulus [38]. Locally resonant bandgaps and nearly perfect absorption can appear near the negative mass or modulus band.

Acoustic metasurfaces can induce wave phase gradient along the interface to tactically adjust the reflection and refraction of sound waves [39, 40]. Many metasurfaces take the form of space-coiling structures [41, 42] combined with perforated plates [43] to induce local resonant effects, enabling highly efficient sound insulation [44, 45] and absorption [46]. Acoustic metamaterials designed based on coordinate transformation theory [47] can deliver cloaking effect [48], as shown in Fig. 2e. This theory, firstly proposed in 2006 [49], provides an equivalent relationship between spatial transformation and material distribution [50, 51], which can be realized with pentamode materials [52, 53]. Recently, metamaterials or phononic crystals with topological states have attracted overwhelming attention [54, 55]. Topological states enable robust one-way sound transport [56–58], construction of topological insulators [59–61] and topological semimetal [62, 63], or acoustic valley Hall effects [64] and Weyl points [65]. All these unusual properties enabled new devices, meta-structures, or sensors for controlling vibration, noise, surface wave and wave vectors [66].

Beyond those linear acoustic metamaterials, *nonlinear acoustic metamaterials* (NAMs) represent a novel class of nonlinear periodic structures distinguished by their remarkable sup/sub-harmonic characteristics. Before delving into details, we broaden our perspective on nonlinear periodic structures and briefly revisit their development over the past seven decades. Across various disciplines, the FPUT chains and granular crystals have played pivotal roles in aiding our exploration and comprehension of nonlinear phenomena within diverse physical systems.

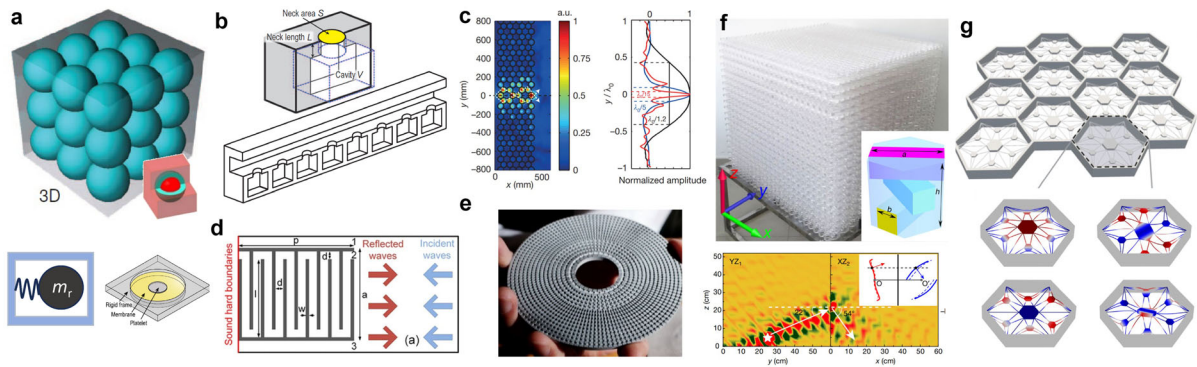


Fig. 2 Typical acoustic metamaterials. **a** Locally resonant meta-cell and its equivalent model. Locally resonant metamaterial consisting of three-components resonators. Membrane resonators for constructing metamaterial. **b** Metamaterial consisting of arrays of Helmholtz resonators [38]. **c** Metamaterial

with negative refraction [43]. **d** Acoustic meta-surface. **e** Acoustic cloaking [48]. **f** Topological metamaterial with negative property [65]. **g** Multi-band gap metamaterial with electrospun spider-web resonators embedded in a 3D printed honeycomb [66]

2.2 FPUT chains and granular crystals

In 1955, Fermi, Pasta, Ulam and Tsingou (FPUT) numerically studied wave propagation in a chain involving weak nonlinear interaction between the oscillators [67]. The chains with quadratic and cubic forces are called α -FPUT and β -FPUT models, respectively. The equation of motion for the n^{th} particle writes:

$$\ddot{x}_n = (x_{n+1} + x_{n-1} - 2x_n) + \alpha \left[(x_{n+1} - x_n)^2 - (x_n - x_{n-1})^2 \right] \quad (2)$$

$$\ddot{x}_n = (x_{n+1} + x_{n-1} - 2x_n) + \beta \left[(x_{n+1} - x_n)^3 - (x_n - x_{n-1})^3 \right] \quad (3)$$

Under long-wave assumption, they can be transformed into the following wave equations:

$$\begin{aligned} \alpha - \text{model} : \quad \frac{\partial^2 u}{\partial t^2} &= \frac{\partial^2 u}{\partial x^2} + \alpha \frac{\partial u}{\partial x} \frac{\partial^2 u}{\partial x^2} \\ \beta - \text{model} : \quad \frac{\partial^2 u}{\partial t^2} &= \frac{\partial^2 u}{\partial x^2} + \beta \left(\frac{\partial u}{\partial x} \right)^2 \frac{\partial^2 u}{\partial x^2} \end{aligned} \quad (4)$$

The above two wave equations can represent many nonlinear crystals or matters [68, 69].

Under an initial pulse input, it was a common belief that any nonlinearity in these models would lead to ergodicity among multiple modes, which spreads energy to higher harmonics [3]. However, Fermi, Pasta, Ulam and Tsingou found that the energy in the weakly nonlinear chain can completely go back to the

first mode after a sufficiently long time. This recurrent behavior that seems to prevent the chain from reaching thermal equilibrium is referred to as the FPUT paradox [1]. Subsequent studies on the FPUT paradox sparked formidable developments in nonlinear science. Topics include integrability of nonlinear differential equations, stability of solutions, chaos, breathers (a type of stable localized nonlinear oscillation), solitons, Bose-Einstein condensation, and even quantum chaos [70–75]. Recently, Refs. [68] proposed a feasible method to search the discrete breathers in a 2D triangle β -FPUT lattice, and reported several 2D breathers with frequency bifurcation from the upper edge of the phonon band. In diatomic FPUT chains, Ngamou et al. [76] showed the super-transmission phenomenon; Chaunsali et al. [70] observed nonlinearity-induced edge states bifurcating from the bulk soliton solutions.

In the 1980s, numerous theoretical studies on FPUT-like models and nonlinear differential wave equations required the materialization of elastic systems for experimental validations. A prime example is the experimental setup built upon granular crystals [77, 78], which consists of arrays of spherical particles

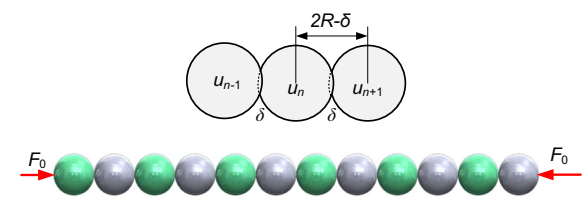


Fig. 3 Model of granular crystal

[5], as depicted in Fig. 3. Nesterenko et al. systematically investigated granular chains, revealing unique nonlinear behaviors [79]. Over more than two decades between 1990 and 2015, solitons [80–82], breathers [83, 84], bandgaps, nonreciprocity, dispersion properties [29] in granular crystals, especially in 1D system, were thoroughly examined. In addition to granular crystals, other studies on nonlinear periodic structures and crystals have also shown intriguing wave phenomena, including slow Bragg solitons [6], intensity-dependent response [85], switching and chaotic dynamics [86], modulational instability [7, 87], second-harmonic generation [88], etc.

2.3 Typical models and designs of nonlinear acoustic/elastic metamaterials

The focus of nonlinear periodic models has primarily been on FPUT-like systems, which exhibit Bragg bandgaps and weak nonlinearity, as clearly illustrated in Fig. 4c. Nevertheless, the majority of studies focusing on FPUT models have been confined to the low-frequency band, where a constant wave speed is assumed alongside the long-wave approximation. Consequently, the intricate properties of the bandgap and the profound impacts of dispersion behavior remain largely unexplored.

Upgrading from FPUT models, we define *nonlinear acoustic metamaterials (NAMs) as artificial composite materials or structures featuring unusual low-frequency, subwavelength nonlinear wave properties*. These properties go beyond (or give new dimensions on) the negative effective mass/modulus, low-frequency bandgaps, wave absorption/insulation/reflection, phase modulation, cloaking and topological propagation found in their linear counterparts.

The simplest NAM model is a 1D diatomic chain shown in Fig. 4b. Nonlinear interactions can be tactically imposed in the primary chain, in local resonators or in both. For convenience, here we classify the NAM models into three types: R-type models include nonlinear interaction only in local resonators while the primary chain is linear; P-type models include nonlinear interaction only in the primary chain, with local resonators being linear; RP-type models include nonlinearity in both. For the diatomic model, the equations of motion of the n^{th} metacell are

$$\begin{aligned} R\text{-model: } & \begin{cases} m_0 \ddot{x}_n = k_0(x_{n+1} + x_{n-1} - 2x_n) + k_r(y_n - x_n) + \{F_{\text{NR}}(y_n - x_n)\} \\ m_r \ddot{y}_n = -k_r(y_n - x_n) - \{F_{\text{NR}}(y_n - x_n)\} \end{cases} \\ P\text{-model: } & \begin{cases} m_0 \ddot{x}_n = k_0(x_{n+1} + x_{n-1} - 2x_n) + k_r(y_n - x_n) \\ \quad + \{F_{\text{NP}}(x_{n+1} - x_n) - F_{\text{NP}}(x_n - x_{n-1})\} \\ m_r \ddot{y}_n = -k_r(y_n - x_n) \end{cases} \end{aligned} \quad (5)$$

Here, m_0 and m_r are the masses of the primary oscillator and local resonator, respectively; k_0 and k_r are their linear stiffness coefficients; $F_{\text{NR}}(\Delta)$ or $F_{\text{NP}}(\Delta)$, denotes the nonlinear force as a function of the displacement difference Δ . It can be a quadratic, cubic, piecewise, or described by other nonlinear functions. In a broader view, nonlinear metamaterials can have local or global nonlinear stress–strain (σ – ε) relationships like $\sigma = E_1 \varepsilon + E_2 \varepsilon^2 + E_3 \varepsilon^3$. If E_n for $n > 1$ is large or the dynamic deformation is large, the effective parameters of E_{eff} or m_{eff} may change greatly, which would drastically change the wave dynamics. The discrete model can be rewritten in the form of coupled differential equations, or in the form of wave equation by using equivalent mass density ρ_{eff} and stiffness k_{eff} ,

$$\begin{aligned} \rho_{\text{eff}} \frac{\partial^2 u}{\partial t^2} + k_{\text{eff}} \frac{\partial^2 u}{\partial x^2} \\ + N \left(\frac{\partial u}{\partial x} \right)^n \left(\frac{\partial^2 u}{\partial x^2} \right)^m \left(\frac{\partial^2 u}{\partial x \partial t} \right)^p \left(\frac{\partial u}{\partial t} \right)^q \\ = f(x, t) \end{aligned} \quad (6)$$

Here N denotes nonlinear coefficient; and one can adjust n , m , p , q to characterize different types of nonlinearities. As shown in Fig. 4d, the linear diatomic model has a low-frequency, subwavelength, locally resonant bandgap. The appearance of nonlinearity changes the properties of “bandgap” (if exists) and wave propagation (Fig. 4). The growing interest is underpinned by the increasing complexity of the problem and the opportunities it offers.

Up to now, several types of nonlinear acoustic metamaterials (NAMs) have been proposed, each with unique characteristics and application promise. Theoretically, any metamaterial can exhibit nonlinear behavior if the input amplitude or intensity is sufficiently high. This principle underlies the first type of NAM, which involves the introduction of high-intensity sound (> 140 dB) into acoustic waveguides, such as arrays of sound cavities or resonators, like the tube in Fig. 2b. These cavities or resonators produce locally resonant effects, and nonlinearity is triggered by the

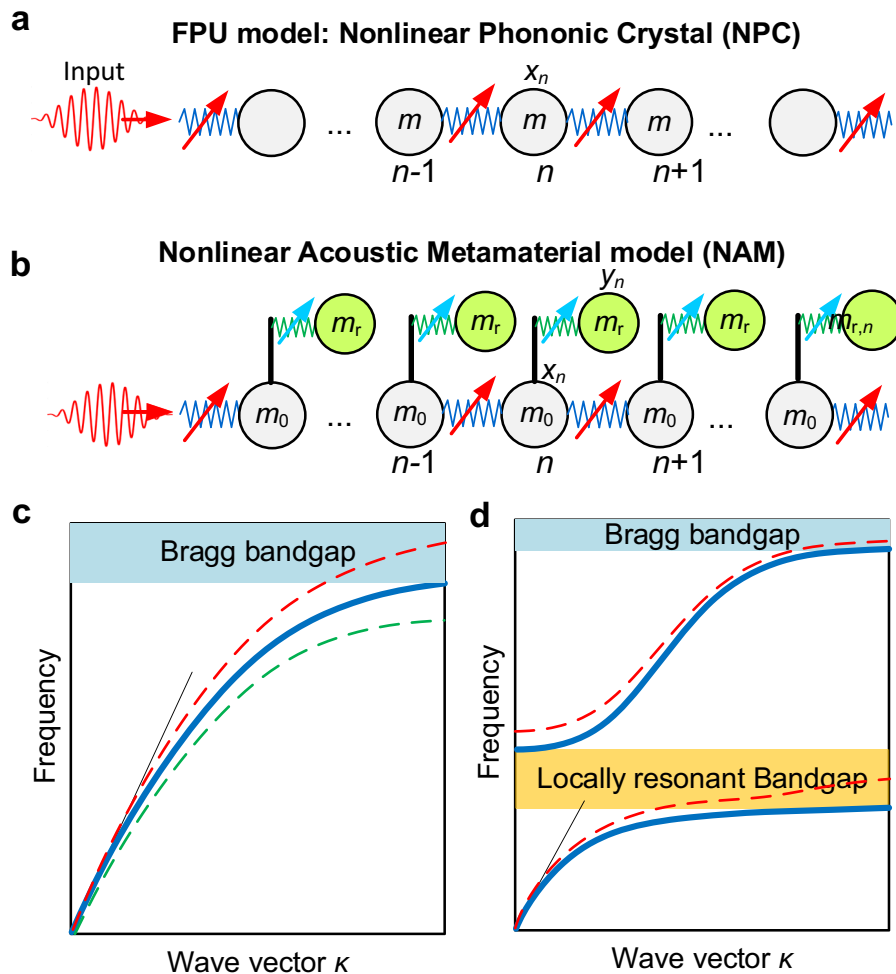


Fig. 4 Crystal and metamaterial models. **a** Fermi-Pasta-Ulam-Tsingou (FPUT) chain model: Also, a classical nonlinear crystal model. **b** Diatomic nonlinear metamaterial model. **c** Dispersion

curve of the linear mono-atomic chain. **d** Dispersion curves of the linear diatomic metamaterial. Dashed curves in (**c**, **d**) illustrate the shifting induced by nonlinearity

high-intensity sound. This approach falls into the realm of nonlinear acoustics problems and has been studied by researchers like N. Sugimoto in the early 1990s [93, 94], followed by Bradley [95–97], and more recently in Refs. [98, 99]. It is worth noting that acoustic nonlinearity that can be practically achieved is generally weak, so it is challenging to generate sound pressures exceeding 150 dB in practice.

Similar with the first type, the second type involves geometrical nonlinearity of the metacell structures, or uses the material nonlinearity of metacell materials. For example, the mechanical metamaterials consisting of rigid units and elastic hinges can have weak geometrical nonlinear effects under large amplitude input [100]. The 2D NAM proposed by Lacarbonara

[66, 101] shown in Fig. 2g is a 3D-printed honeycomb hosting electrospun spider-web resonators which exhibits various nonlinear local resonances associated with the hardening membrane stretching nonlinearity and the softening material nonlinearity of the CNT/PVDF electrospun spider webs. Based on geometrical nonlinearity, one can induce bistable, multi-stable nonlinearity in resonators using buckling elements [102, 103]. Except for the quasi-static properties such as shape morphing [104, 105], energy absorption [106, 107], multi-stable metamaterials also support interesting nonlinear wave dynamics.

The third type of NAM utilizes magnetic or electrostatic forces to generate nonlinear stiffness. This approach was explored by Fang et al. in 2017 [23]

(Fig. 5c). More recently, Cha and Daraio proposed a nanomechanical NAM array controlled by electrostatic force [92], as shown in Fig. 5e,f. However, both magnetic and electrostatic interactions tend to exhibit weak nonlinearity under dynamic input, limiting their effectiveness in certain applications.

As the field of NAMs continues to evolve, researchers are exploring new methods to achieve enhanced nonlinearity and broaden the range of potential applications. Many previously mentioned investigations indeed highlight that, without a deliberate design to achieve enhanced nonlinearity, metamaterial structures tend to exhibit only weak nonlinear behavior. Generating sufficient nonlinear effects in such designs often requires extremely large amplitudes. Introducing strongly nonlinear metamaterials has demonstrated remarkable ultra-low and ultra-broad performance characteristics [23]. As shown in Fig. 5a, b, the core of this NAM design involves a beam or plate as the primary structure, upon which nonlinear resonators are periodically installed. Each metacell comprises a cluster of magnets connected by rods. The repulsive force between these magnets introduces a weak level of nonlinear interaction. The important feature of this design is the clearance left between the center magnet and the rod. This gap enables a vibro-impact motion between the magnet and the rods during flexural vibrations, leading to a strong nonlinear response. In fact, the weak geometric nonlinearity inherent in these NAMs is essentially negligible compared to the strong chaotic effects induced by the coupled vibro-impact oscillators.

Furthermore, other NAM designs incorporating coupled vibro-impact resonators have been explored to reveal novel wave phenomena [27, 108]. For instance, Sheng et al. [90, 91] developed a metacell that exhibits dual vibro-impact resonances in both vertical and transverse directions. This design not only enhances nonlinearity but also allows for more complex wave interactions. Additionally, the deformation of microstructures within these metamaterials has been shown to enable strong nonlinearity [108], further broadening the range of potential applications.

Therefore, despite the efforts made, the available practical methods for generating and enhancing nonlinearities in compact NAMs are still limited. This calls for more innovative and concerted efforts as further research work.

3 Properties of wave propagation in nonlinear acoustic metamaterials

Properties of NAMs are reviewed in this section. Nonlinear periodic crystals (NPCs) are also mentioned in a broader view. The comprehension of the role played by bandgaps in NAMs and NPCs is the key to understanding their unique wave propagation properties. Therefore, nonlinear bandgap is the mostly studied feature, which, a priori, relies on the calculation of dispersion curves.

3.1 Calculation methods of nonlinear dispersion and bandgaps

As most metamaterials are periodic structures, calculating their bandgaps in linear systems relies on Bloch-Floquet theorem expressed as

$$\varphi(\mathbf{r} + \mathbf{R}_n) = e^{i\mathbf{k} \cdot \mathbf{R}_n} \varphi(\mathbf{r}) \quad (7)$$

Here $\varphi(\mathbf{r})$ is the wave field in the reference unit cell; \mathbf{r} denotes the coordinate vector inside this unit cell; \mathbf{R}_n is the Bravais lattice vector crossing n unit cells from the reference cell; \mathbf{k} denotes the wave vector in Brillouin zones.

We note that the Bloch-Floquet theorem was established based on linear transformation, applicable to linear systems in which both geometrical and dynamic periodicity exists. It describes the linear mapping relation between the wave fields of two cells. Strictly speaking, it cannot be applied to nonlinear periodic systems, since although geometric periodicity still exists, the dynamic periodicity is destroyed due to the amplitude-dependent features of the nonlinear oscillators. Having said that, there is no such succinct nonlinear mapping function for nonlinear periodic systems at present. Therefore, except for the direct numerical method, Bloch-Floquet theorem can still be applied to some extent with precaution to provide reasonable approximate results for nonlinear periodic systems. Nevertheless, we emphasize that the predictions of this theorem are wrong for “far” fields, which will be expounded in Sect. 3.3, where a self-adaptive framework is provided. Here we first focus on calculation methods.

With the Bloch-Floquet theorem and proper modelling methods (e.g., finite element method), the

nonlinear equations of motion of a single nonlinear unit cell read:

$$\mathbf{M}\ddot{\mathbf{u}} + \mathbf{K}\mathbf{u} + \mathbf{f}_{\text{NL}}(\mathbf{u}) = 0 \quad (8)$$

where \mathbf{M} and \mathbf{K} are the linear mass and stiffness matrices, respectively; \mathbf{u} is deformation vector; and $\mathbf{f}_{\text{NL}}(\mathbf{u})$ denotes the deformation-dependent nonlinear function. Several approaches were established to solve the nonlinear dispersion equations.

The perturbation approach allows for closed-form determination of the effects exerted by weak nonlinearities on dispersion and group velocity [109]. For the commonly adopted cubic nonlinear system with $\mathbf{f}_{\text{NL}}(\mathbf{u}) = \mathbf{N} \cdot \mathbf{u}^3$, the perturbation solution of dispersion relation writes [20, 109]

$$\omega = \omega_0 + \frac{3A_0^3 \mathbf{u}_{0j}^H(\mathbf{k}) \mathbf{N} [\mathbf{u}_{0j}^2(\mathbf{k}) \mathbf{u}_{0j}^*(\mathbf{k})]}{8A_0 \omega_{0j} \mathbf{u}_{0j}^H(\mathbf{k}) \mathbf{M} \mathbf{u}_{0j}(\mathbf{k})} + O(\varepsilon^2) \quad (9)$$

where ω_0 denotes the frequency solution of linearized system for specified wave vector \mathbf{k} ; \mathbf{u}_{0j} is the eigenvector of j^{th} eigenvalue ω_{0j} ; A_0 denotes the wave amplitude at a point. Specially, for a diatomic model with an acoustic branch and an optical branch, the expressions are written in the form [101, 110]:

$$\begin{aligned} \omega_{nl}^- &= \omega^- + \frac{3(\phi_2^-)^4}{8\omega^-} N_3 [(a^-)^2 + 2(a^+ \phi_2^+ / \phi_2^-)^2] \\ \omega_{nl}^+ &= \omega^+ + \frac{3(\phi_2^+)^4}{8\omega^+} N_3 [(a^+)^2 + 2(a^- \phi_2^- / \phi_2^+)^2] \end{aligned} \quad (10)$$

where ω_{nl}^\pm and ω^\pm denote the nonlinear and linear frequencies of the acoustic (-) and optical (+) modes, respectively; (ϕ_1^\pm, ϕ_2^\pm) and a^\pm the corresponding optical/acoustic wave eigenmodes and their amplitudes; N_3 is the nonlinearity coefficient. The above closed-form expressions allow to study the nonlinear bandgap ($\omega_{nl}^+ - \omega_{nl}^-$) and the dependence on the amplitudes as well as the hardening ($N_3 > 0$) or softening ($N_3 < 0$) nonlinear local resonances of the resonators.

The perturbation method is widely used studying weakly nonlinear phononic crystals and metamaterials, including the granular crystals, 1D model [109, 111] to 2D lattices [112–114]. Early contributors include Narisetti, Fang, and Manktelow. Fortunati et al. [115, 116] employed a Hamiltonian perturbation method together with Lie series for a diatomic NAM

model, and studied the invariant manifolds of 2:1, 1:1 and 3:1 auto-parametric resonances between acoustic and optical branches.

However, the perturbation solution gives wrong results for moderately and strongly nonlinear systems (large nonlinear coefficients or high amplitudes). In this case, results from the harmonic balance method and homotopy method provide more reasonable results without curled dispersion curves. The harmonic balance method [111, 117] delivers the dispersion solutions of the following characteristic equations:

$$[\mathbf{K} - \omega^2 \mathbf{M}] \mathbf{U}(\mathbf{k}) + \mathbf{f}_{\text{NL}}(\mathbf{U}) = 0 \quad (11)$$

By specifying the value of an element in vector $\mathbf{f}_{\text{NL}}(\mathbf{U})$, we can obtain the frequency ω and other features.

Furthermore, the homotopy method was proposed to analyze the bandgaps of NAMs, which is applicable to both weakly and strongly nonlinear systems [20, 21]. With the homotopy method, a linear operator $L(\mathbf{f})$, a nonlinear operator $N(\mathbf{u}, \Lambda)$, and a homotopy $H(\mathbf{u}; q, \mathbf{H}_0)$ are defined using the original equations of motion:

$$\begin{aligned} L(\mathbf{f}) &= \frac{d^2 \mathbf{f}}{d\tau^2} + \phi \mathbf{f}, \quad N(\mathbf{u}, \Lambda) = \Lambda^2 \mathbf{M} \frac{\partial^2 \mathbf{u}}{\partial \tau^2} + \mathbf{K} \mathbf{u} + \mathbf{f}_{\text{NL}}(\mathbf{u}, \mathbf{u}') \\ H(\mathbf{u}; q, \mathbf{H}_0) &= (1 - q)L(\mathbf{u}(\tau, q) - \mathbf{u}_0(\tau)) - q\mathbf{H}_0 \cdot N(\mathbf{u}(\tau, q), \Lambda(q)) \end{aligned} \quad (12)$$

Giving the initial solution \mathbf{u}_0 and a proper auxiliary quantity \mathbf{H}_0 , we can obtain the high-order solution by making parameter q increase from 0 to 1; here $\Lambda(q)$ is the variable relevant with frequency ω , $\tau = \omega t$. The initial solution can be identical with the first-order harmonic balance solution.

Furthermore, an analytical homogenized method was established in [118] by combining the bifurcation of nonlinear local resonances. For a metacell containing a local resonator with cubic nonlinearity, its effective mass m_{eff} writes

$$m_{\text{eff}} = m_0 + \frac{k_r + 3k_n U_r^2 / 4}{\omega_r^2 - \omega^2 + 3k_n U_r^2 / (4m_r)} \quad (13)$$

Here U_r is the vibration displacement of the nonlinear local resonator calculated from the equations of motion of a unit cell, which gives the bifurcation plots; other parameters are identical with those defined in Eq. (1). This expression is the same as

that of Eq. (1) if the nonlinear stiffness coefficient vanishes, i.e., $k_n = 0$. If the metamaterial substrate is a beam, we can obtain the wave number based on m_{eff} ,

$$k(\omega) = \left[\left(m_0 + \frac{k_r + 3k_n U_r^2/4}{\omega_r^2 - \omega^2 + 3k_n U_r^2/(4m_r)} \right) \frac{\omega^2}{D_0 V_{\text{cell}}} \right]^{\frac{1}{4}} \quad (14)$$

As demonstrated in [27], the homogenized method based on the bifurcation of nonlinear local resonances is also effective for the metacells containing multiple nonlinear resonators. Equations (13,14) clearly show the relationships among nonlinear local resonance, effective mass density, bandgaps and passbands [118], thus highlighting the essential features by including nonlinearity in metamaterials. This method shows that a nonlinear bandgap starts from the saddle-node bifurcation of nonlinear local resonance, a finding that can promote insights into complex band behaviors [27].

Besides the discussed analytical methods, for the 1D model, numerical spectra-spatial [119] analyses of dispersion curves using 2D Fourier transform can provide accurate information about the nonlinear dispersion curves.

3.2 General properties of nonlinear bandgaps: amplitude dependence

It is crucial to note that the linear bandgap of some nonlinear periodic structures can be dynamically adjusted by altering external fields or forces. For instance, the bandgap of a nonlinear nanomechanical lattice, as depicted in Fig. 5e, can be shifted from 14 to 16 MHz by adjusting the static voltage [92]. This tunable nature is reminiscent of the way of granular crystals that can enhance their sound speed and broaden their bandgap by applying precompression [120]. The pre-compressive force in these systems can also be imposed using a magnetic field, providing another means of tuning the bandgap [121, 122]. However, active tunability does not necessarily involve nonlinear dynamics.

Typical responses and dispersion curves of the diatomic NAM model are shown in Fig. 6a, b. Similar to other general nonlinear dynamic effects, the bandgaps in NAMs and NPCs exhibit a pronounced amplitude-dependence. As the wave amplitude

increases, the bandgaps in a NAM undergo complex variations such as shifting, switching, and even coupling, as evident in Fig. 6c, d. This amplitude-dependent bandgap behavior is one of the most extensively studied characteristics of NAMs. Furthermore, the directionality of these changes is closely linked to the type of nonlinearity involved. For instance, in the case of softening nonlinearity, the bandgap shifts downward with increasing amplitude [110], while for hardening nonlinearity, it shifts upward [123].

The shifting leads to a broader “bandgap” in theory [21]. From a different perspective, wider bandwidth can be regarded as a consequence of the bending of the backbone curves to the left or right of the linear natural frequency [101, 110]. The bending of the backbone curves, driven by nonlinear stiffness variations with oscillation amplitude, produces a broader resonance branch. However, excessive nonlinearity might lead to the disappearance of some bandgaps. Furthermore, adjusting the width and frequency of locally resonant and Bragg bandgaps through amplitude modulation [20, 22], entailing a transition from separation to adjacent coupling between them [124].

Studies have explored amplitude-dependent bandgap phenomena in various NAM models. For discrete NAM models, studies encompass different chains with various nonlinearities, including the R-type (diatomic, triatomic and four-atomic) models [125–127], P-type models [128, 129], chains with bilinear nonlinearity [124] and quadratic nonlinearity [130, 131], with inertia amplification metacells [132] or nonlinear inertance resonators [133], with nearly zero bandgap frequency [134]. For continuous systems, relations among nonlinear local resonance, effective mass density, bandgaps and passbands are clarified based on the NAM beam [118]; Richoux et al. [135] investigated how nonlinearity in periodic Helmholtz resonators affects the cutoff frequency of dispersion bandgaps in pipelines. Additionally, Ref. [136] analytically examined nonlinear bandgaps in waveguides composed of Helmholtz resonators and membranes, which exhibit concurrent negative modulus and density. Lan et al. [137] further explored the nonlinear acoustic impedance and equivalent mass of this structure, revealing that strong nonlinearity shifts the bandgap to lower frequencies. In other views, Bilal et al. [138] generated geometric nonlinearity through the coupling of oscillators and magnetic forces,

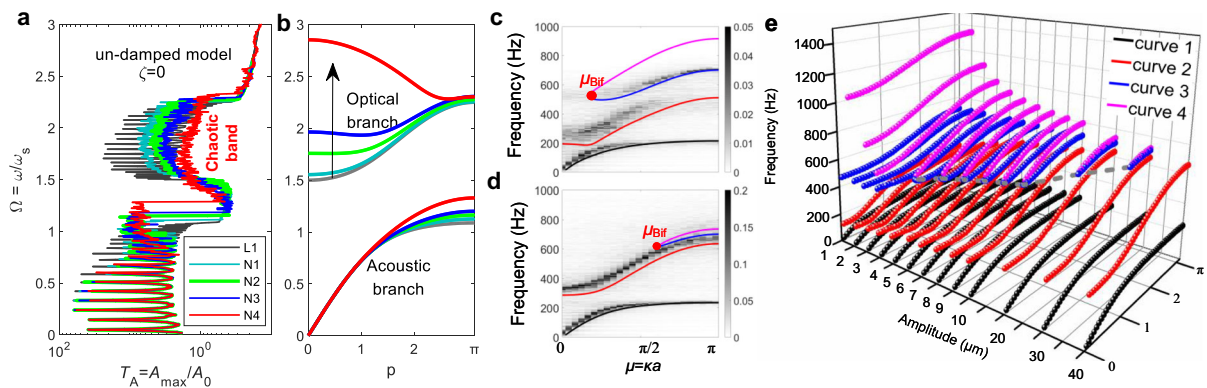


Fig. 6 Bandgap properties of nonlinear metamaterials. **a**, **b** Frequency responses (**a**) and dispersion curves (**b**) of diatomic NAMs with different nonlinear coefficients [21]. **c–e** Band degeneration of a triatomic NAM model with increasing

incident amplitude A_0 . [25] **c** Moderate nonlinearity ($A_0 = 5 \mu\text{m}$), **e** Strong nonlinearity ($A_0 = 30 \mu\text{m}$). **e** Overall view of analytical dispersion curves varying with increasing amplitude A_0

realizing a phonon switch element similar to a transistor; Lou et al. [139] used softening or hardening nonlinear metamaterials to block the propagation of Rayleigh waves in a linear solid.

These studies covered most NAM types and clarified general amplitude-dependent properties: bandgap shifting, coupling and transition. This greatly impacts the band-edge modes, and shifts the transient wave frequency [119]. Recently, a combination of linear and nonlinear metamaterials has demonstrated amplitude-activated passive direction-bias in wave propagation [140], originating from bandgap shifting. Based on the asymptotic solutions in Eq. (10), Shen and Lacarbonara investigated nonlinear dispersion properties of a metamaterial beam and a 2D metamaterial honeycomb embedding spider web-like resonators [101, 110], as shown in Fig. 2g. This model can behave as a hardening or softening nonlinear NAM, controlled by the modal mass and modal stiffness, and both induce apparent bandgap shifting [110], as shown in Fig. 7. This benefits optimization design. The nonlinear bandgap gain remains greater than 1 across the entire wave amplitude range (Fig. 7b), offering a 60% increase of the bandgap for specified amplitude (Fig. 7c).

Except for the amplitude-dependent properties, the sub-harmonic or super-harmonic internal resonances are the most salient and interesting features of nonlinear systems for triggering energy transfer. In this regard, Silva et al. [26] studied a NAM model considering nonlinear hyperelastic interactions between a rubber-like elastomeric local resonator

and the hosting matrix. This model, due to a 2:1 internal (auto-parametric) resonance, generates a complementary 1/2 sub-harmonic attenuation zone alongside the local resonance bandgap. For a diatomic NAM model, M. Lepidi and A. Bacigalupo [141] demonstrated that perfect 1:1 internal resonance could not occur due to the gap between the acoustic and the optical bands, different from super-harmonic 3:1 internal resonance that could take place within a frequency range. These preliminary studies about internal resonance in NAMs show unusual properties of nonlinear systems, and we think it worth further exploration.

In bistable or multi-stable metamaterials [142, 143], the negative stiffness underlies distinct mechanisms that govern wave propagation and can serve as a powerful bandgap modulator [144–146]. Low-frequency and broadband wave attenuation can be realized by shifting the initial frequency of the bandgap to nearly zero through tuning the wave amplitude to a critical value [147].

As reviewed above, the general properties of NAM bandgaps have been examined in many 1D models. Though one can inspect weakly nonlinear bandgaps in 2D and 3D models directly using perturbation approach and linear band theory, little effort was made on studying strongly nonlinear bandgaps in 2D models and nearly nothing on 3D models. This will encounter difficulties in finding dispersion solutions of high-dimensional algebraic equations based on the harmonic-balance frame, and also in determining physical meaning of multiple solutions near a

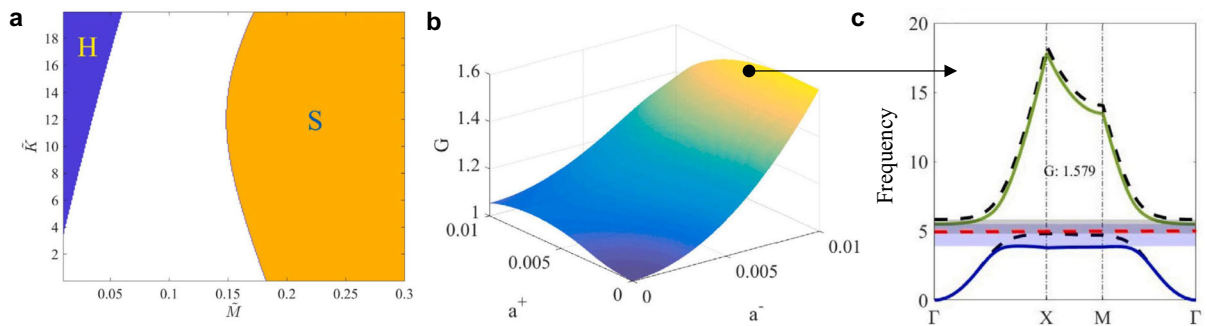


Fig. 7 Optimal 2D NAM design for wave control [101]. **a** Resonator design chart depicting regions of optimal (orange) softening resonator nonlinearity and (blue) hardening nonlinearity as a function of their modal mass and modal stiffness;

b Nonlinear bandgap gain vs. acoustic/optical wave amplitudes for a softening resonator indicated by the red diamond in (a); **c** linear (dashed lines) vs. nonlinear bandgaps (blue and green lines) for given wave amplitudes

dispersion curve. Moreover, studying the influences of amplitude-dependent bandgaps on wave propagation requires direct time-domain simulations or improved frequency-domain approaches, which in both cases, is time-consuming and needing better integration algorithms. For finite metamaterial models, this is possible even for the large-scale NAM plate containing hundreds of nonlinear resonators by combining frequency-domain methods and continuation approach [89]. Therefore, solving these problems also calls for highly efficient calculating methods. Furthermore, nonlinear bandgaps may enable novel wave phenomena and advanced functionality, especially in quickly updating metamaterials for reconfigurability, wave phase control, sound absorption and topological propagation.

3.3 Band degeneration and self-adaptivity:

Essential process of bandgap transformation

The subharmonic and super-harmonic bandgaps go beyond the amplitude-dependent bandgap shifting. However, in above studies, amplitude-dependent bandgaps in NAMs and NPCs were shown to exhibit shifts as “linear” bandgaps [148], consistent with predictions obtained using the Floquet-Bloch theorem. However, this theorem rests on two key assumptions: *stationary invariance* and *space-time invariance*. Stationary invariance assumes that the dispersion curves shift with amplitude, akin to varying stiffness coefficients, while maintaining the same number of curves and wave modes in the band graphs. Space-time invariance assumes that these curves and

bandgaps remain constant across propagation space and time.

Unfortunately, these assumptions are not universally valid, particularly for models with moderate to strong nonlinearity. To inspect the stationary invariance, Gong et al. [25] tracked the evolution of the band structures of a strongly nonlinear triatomic NAM model based on harmonic balance method and spectral-spatial analyses. Results showed that, under moderate nonlinearity, dispersion curves can merge, bifurcate, shorten, or disappear, leading to incomplete or entirely vanished bands. This process of band degeneration occurs in different and rather complex manners depending on the arrangement and the coupling of nonlinear elements. As nonlinearity increases, the dimension of the unit cell, bandgap range, and mechanisms (Bragg and local resonance) all vary with amplitude, indicating a change in wave modes. Therefore, the stationary invariance of band structure, as conventionally understood, does not hold for NAMs and nonlinear phononic crystals with moderate to strong nonlinearity. This finding is crucial for accurately predicting and controlling wave propagation in these complex nonlinear systems. Future studies should carefully consider the impact of nonlinearity on band structure and wave modes to ensure reliable predictions and designs.

Moreover, let us delve deeper into the applicability of “space-time invariance” implied by Bloch theorem in NAMs. Using a NAM beam model, Fang et al. [118] first found that the nonlinear local resonant bandgap corresponds to a distance-amplitude-dependent behavior that leads to a self-adaptive bandwidth in the far field. Later on, they [27] reported a rigorous

analytical, numerical and experimental demonstration of the self-adaptive band and self-broadening bandgap with a triatomic NAM containing enhanced nonlinear interaction, as shown in Fig. 8. For the NAM without any external active control, they found that its bandgap effect can adaptively broaden as the propagation distance/time increases, *i.e.*, the adaptive-broadening bandgap, which also dominates the broadband acoustic limiting for blocking 97% of energy.

In essence, this self-action underscores the fact that the band structure of nonlinear periodic structures is not merely amplitude-dependent but also distance/time-dependent. In other words, the assumption of “space–time invariance” inherent in the Bloch theorem cannot be universally applied to nonlinear structures. Nevertheless, it can still provide valuable insights into predicting local attenuation within specific regions of these nonlinear structures or materials, but need to be used with extreme caution. This revelation has profound implications for the design and application of NAMs.

Mechanisms for this self-adaptivity are clarified [27]. It is also relevant to the amplitude-dependent bandgap. Harmonic generation and chaotic responses

play key roles in triggering the adaptive process even without damping. Then, bandgap effect appears at the surface or inside some positions of NAM, resulting in significant wave attenuation (see Fig. 8d). Chaotic responses and nonlinear bandgap strengthen the attenuation cyclically. Moreover, in experiments, the bandgap effect overcomes the limitation of the mass ratio for conventional locally resonant bandgaps in linear metamaterials. The self-adaptive bandgap is a general feature on NAMs even in periodic bistable structures [147].

Based on our experience, we think bandgaps’ self-adaptivity, instead of the normal amplitude-dependent shifting, dominates the wave propagation in strongly nonlinear systems or the NAM consisting of multi-degree-of-freedom resonators. However, this is not well recognized, and its influences on wave propagation in 2D and 3D NAMs remain unveiled. Studying this feature should base on a large-scale model and creating non-reflection boundary conditions, which may bring difficulties in numerical integration.

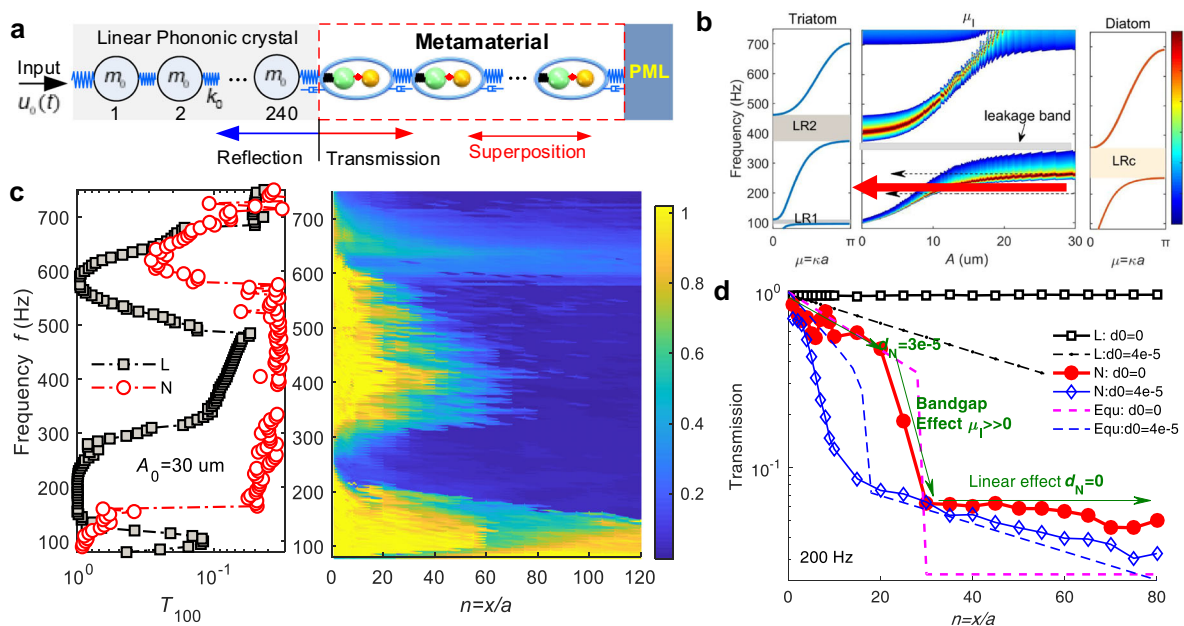


Fig. 8 Self-adaptive band and self-broadening bandgap [27]. **a** Numerical model of triatomic NAM model. **b** Amplitude-dependent bandgap of the triatomic NAM. The first and third insets are dispersion curves of the triatomic and diatomic linear counterpart. **c** Wave transmission at different points along the

chain. The left panel shows the transmission at 100th metacell for input amplitude $A_0 = 30 \mu\text{m}$. **d** Wave amplitude change with propagation distance solved with analytical and numerical methods

3.4 Nonreciprocal wave control

Nonreciprocal wave propagation, also termed diode effect [149], offers a one-way route for energy transport [150]. For electromagnetic waves, reciprocity can be violated through imposing an external magnetic field, but it is more difficult for acoustic waves because linear and passive systems lead to reciprocal propagation. Walker et al. [151] reported an experimental observation of linear nonreciprocal transmission of ultrasound in a water-submerged phononic crystal through breaking the P symmetry. Topological states offer non-reciprocity in linear elastic systems by beating time reversibility with active control or external field [56, 60, 65], while it is challenging to do so in broadband and low frequencies. Actively shifting the bandgap of a time-variation metamaterial can break time-reversal symmetry to induce nonreciprocity [152–155]. This essentially induces the space–time modulations [156] as was realized by Chen et al. [157], using a metamaterial beam with a size of $\sim 5\lambda$ and insulation difference of $\Delta T \approx 7$ dB.

Nonlinearity can entail robust nonreciprocal wave transmission, a property that is absent in linear materials without active control [159–161]. In 2004, Li et al. [162] proposed a thermal diode by using two coupled nonlinear lattices. The model is robust in a wide range of system parameters. Recent years have witnessed the extension of the concept to heat conduction [163, 164] and elastic wave manipulation. However, an asymmetric nonlinear system is not sufficient for a nonreciprocal wave diode [165]. Nonreciprocity depends on proper nonlinear models, mechanisms, system parameters, and frequency bands. Several nonlinear mechanisms have been proposed to realize nonreciprocal elastic wave propagation. Here we review the designs, mechanisms, effectivity and diode's size.

In 2005, Nesterenko et al. [82] reported the first experimental acoustic diode of solitary waves using two granular chains triggered by a magnetically induced precompression. The diode effect was materialized by the large gradient of particle velocity near the interface between two segments. Liang et al. [30] proposed an acoustic diode that consists of a segment of linear phononic crystal and a layer of ultrasound contrast agent microbubble suspension, as shown in Fig. 9a. The second harmonic is generated in the

nonlinear medium. The bandgap of the phononic crystal suppresses the fundamental wave while allowing the second harmonic to pass through, leading to an asymmetric transfer of the total energy with a frequency change of the output signal. This mechanism enables a rectifying ratio as high as $\sim 10^4$ by using optimized nonlinear media. The thickness of this diode is typically $\sim 30\lambda$. This mechanism was theoretically analyzed in Ref. [166, 167]. Fu et al. [168] designed a broadband acoustic diode by using an asymmetric bilinear spring as the nonlinear frequency-conversion medium, and using the $1/2$ -order subharmonic wave as asymmetrical energy carrier. Blanchard et al. [160] used Volterra-series based asymptotic analysis to study the non-reciprocity in space for a class of 1D continuous, time-invariant systems with stiffness nonlinearities.

In 2011, Boechler et al. [29] designed an elastic diode using a purely nonlinear granular chain, as shown in Fig. 9b. A defect state is introduced near one end of the granular chain, which generates a nonlinear mode in the passband. When emitting a wave (with frequency in the bandgap) from the defect end, the nonlinear mode is activated by the $1/2$ subharmonic wave, leading to asymmetric energy rectification. This rectifier's length is of the order of 10λ . Inserting asymmetric potential barriers inside the granular chains can also achieve asymmetrical propagation [169]. In 2014, Popa and Cummer [170] demonstrated a non-reciprocal active acoustic diode composed of a single piezoelectric membrane augmented by a nonlinear electronic circuit, and sandwiched between Helmholtz cavities tuned to different frequencies. The design is thinner than a tenth of a wavelength.

As indicated above, nonlinear elastic diodes generally change the output frequency. Gliozzi et al. [171] showed a frequency-preserving elastic diode by mixing several orders of harmonics. Actually, directly using amplitude-dependent nonlinear bandgap can realize frequency-preserved diode effect. Liu et al. [172] proposed a theoretical frequency-preserved diode model formed by coupling a weakly nonlinear periodic structure with asymmetric linear structures at two ends. A similar property was demonstrated using granular crystals [173].

We note that studies should clearly distinguish non-reciprocity of the total energy and that of the fundamental wave. To that end, Ref. [158] theoretically and experimentally demonstrated the frequency-

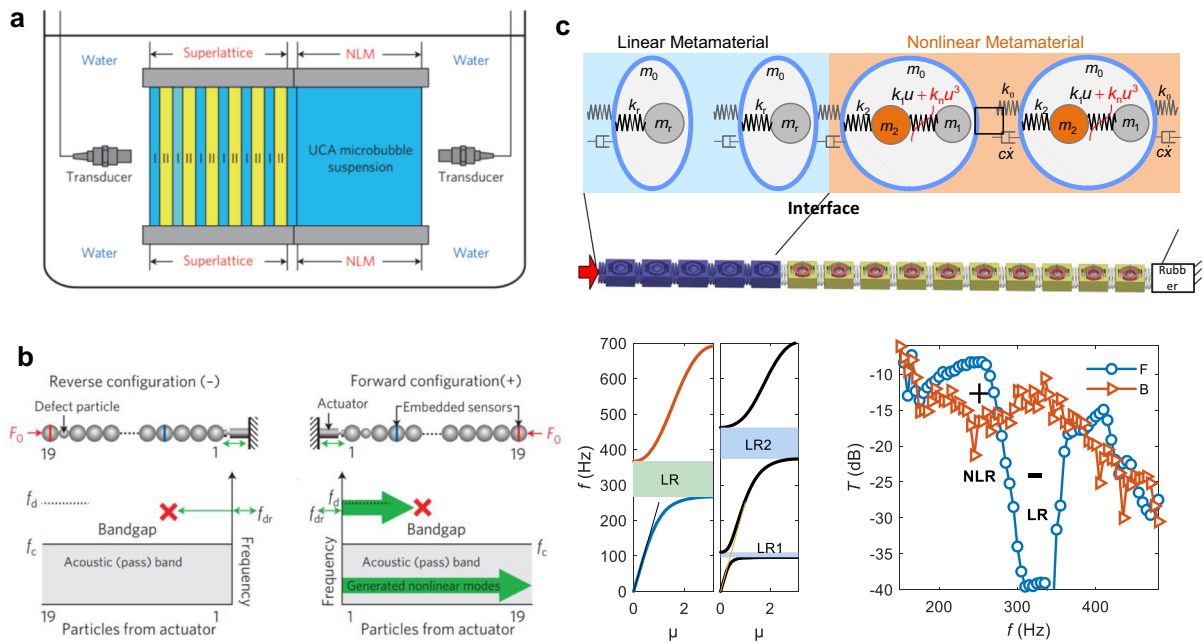


Fig. 9 Nonreciprocal wave propagation enabled by nonlinearity. **a** Acoustic diode consists of a segment of linear phononic crystal and a layer of nonlinear material [30]. **b** Acoustic diode consists of a granular crystal with a defect particle that induces a

nonlinear mode [29]. **c** Bi-directional and frequency-preserving elastic diode consists of a segment of linear metamaterial and a segment of nonlinear metamaterial [158]

preserved, bidirectional, high-quality, low-frequency, subwavelength elastic diode, as shown in Fig. 9c. This has been achieved using an elastic metamaterial with the intentional clearance inside metacells to create enhanced nonlinearity. The corresponding transmission differences in the two bands can reach as much as 20 dB and −40 dB, respectively, while the diode length is of about 1λ . Moreover, they reported three non-reciprocal mechanisms [158]: (i) frequency-preserved nonreciprocity of both the total energy and fundamental wave can be realized by combining the amplitude-dependent bandgap and the interface reflection; (ii) linear bandgap combining with the chaotic responses performs the monochromatic-to-continuous nonreciprocity of total energy, while the propagation of the fundamental wave is weakly nonreciprocal under weak damping; (iii) increasing damping can break the two types of reciprocity from the second mechanism.

These studies manifest that the NAM designs provide new mechanisms and possibilities for realizing nonreciprocal wave control with subwavelength acoustic/elastic diodes. At present, physical mechanisms for realizing nonreciprocal wave propagation

have already been clarified and demonstrated in many systems. Future studies should look into the functions and applications of “acoustic diode” in structures or machines. One may obtain improved targeted energy transfer [174], energy harvester, protected one-way transmission, etc.

3.5 Harmonic generation and manipulation

The most salient nonlinear effect is the harmonic generation. In 1994–1995 [95–97], Bradley investigated the Bloch wave in 1D NPC, and demonstrated that the forward travelling fundamental wave generates both forward and backward traveling second harmonic waves, whose amplitudes oscillate with distance. Scalora et al. [88] described the second harmonic in 1D NPCs, which is then examined by Yun et al. [175] using an extended transfer matrix method. Furthermore, high-order harmonics may lead to jump responses and modal mixing in wave propagation modes [176].

Second harmonic wave will appear in the nonlinear acoustic fields in air when applying high-intense sound (> 140 dB). Therefore, the acoustic metamaterials

consisting of periodically arranged Helmholtz resonators can be used to study the harmonic generation and propagation [28, 177] based on homogenization method. The acoustic metasurface containing coiling-up space can present efficient frequency down-conversions because its Bragg bandgap suppresses the undesired inter-modulation by preventing the propagation of the frequency up-converted harmonics, whereas the coiling-up space amplifies the amplitude of the down-converted waves by decreasing the effective speed of sound [178]. Similar properties of metasurface are also reported in Ref. [179].

Ref. [118] investigated the interaction between fundamental and third harmonic waves in an infinite NAM beam based on analytical and numerical methods. The relative converting efficiency, the amplitude ratio between fundamental and third harmonic, reaches highest in the nonlinear locally resonant bandgap, highlighting the amplification of local resonance for harmonics. Moreover, the propagation of harmonics is essentially different from its fundamental wave. Similar phenomenon is observed in the granular crystal with linear local resonators [180].

As reviewed above, harmonic generation is a salient feature of nonlinear system, but the local resonance in NAM may enhance the converting efficiency, and bandgaps can help to control the propagation and conversion. To improve the significance of high/low-order harmonics, one can conceive special functions and designs for using them. This may need to combine it with the amplitude-dependent bandgap, self-adaptivity, nonreciprocity, breathers, solitons, vibration/wave absorption and insulation, or sound focusing effect [81, 181].

3.6 Chaotic dynamics and chaotic band

Bifurcation and chaos in finite nonlinear periodic structures (including NAMs) have a significant impact on wave propagation, and are much more complex. Bifurcation occurs in various situations. At saddle-node bifurcation point, the solution jumps between quasi-periodic solution branches and chaotic branches [182]. Experimental tests revealed hysteresis loops at the jumping points. Bifurcation can trigger efficient energy transfer to frequencies away from the driving frequency in the transmitted waves [183].

The chaotic responses appear nearly in all strongly nonlinear metamaterials, especially the NAMs

consisting of vibro-impact resonators [184, 185]. Fang et al. conducted systematic investigations on bifurcations and chaos in finite NAM chains by combining the nonlinear dispersion and bandgaps, nonlinear resonances in passbands, and vibration transmission [20–22]. Properties of strongly hyper-chaotic dynamics of 1D NAM were analyzed by examining the stability of periodic solutions, Lyapunov exponents and Lyapunov dimensions. Based on these investigations, they revealed a mechanism for realizing low and broadband vibration suppression—chaotic band [22]. As an example, the chaotic band in a diatomic model is shown in Fig. 6a. The chaotic band is composed of densely nonlinear resonances within the passband. These nonlinear resonances have unstable peaks due to bifurcations, and bifurcations from different resonances interact with neighbors, ultimately leading to hyper-chaos. Additionally, damping has a significant impact on the characteristics of chaotic attractors. For the hardening nonlinear system, the bifurcations and chaos eliminate dense linear resonances above the nonlinear locally resonant (NLR) bandgap. Consequently, the chaos band significantly broadens the elastic wave suppression bandwidth. Subsequent studies on a multi-atomic NAM model showed that the band above the NLR bandgap can become a chaotic band with lower vibration transmission [20]. Increasing the incident amplitude and nonlinear strength can entail greater vibration reduction within the chaotic band. Moreover, the reduction effect is not sensitive to added mass, conducive to achieving broadband vibration reduction with small attached mass [21].

To further control the bandgap and chaotic band, an interesting remote interaction mechanism, termed as bridging coupling of NLR bandgaps, has been discovered and demonstrated [108]. Bridging-coupling is conducive to control of the nonlinear effective mass density and chaotic bands between NLR bandgaps. The bandwidth and efficiency of the wave reduction in chaotic bands can be manipulated effectively by modulating the frequency distance between the bridging pair. The linear bridge-coupling effect was firstly found in Ref. [108] and then systematically studied in Ref. [186].

These preliminary studies show the properties and the remarkable effects of chaos in NAMs. However, due to complexity of the problem and the high dimensional feature of the system, understanding

chaos and bifurcation in NAMs remains very challenging, and important phenomena might be masked and hidden by chaos. Limited advances in chaotic dynamics in high-dimensional systems constitutes a major obstacle for the understanding of chaos in NAMs, especially for finite-scale NAMs with multiple resonances. At present, one can analyze chaotic waves in infinite NAMs that exclude global resonances, and can also establish basic principles based on intensive simulations on finite NAMs (see more in Sect. 4.1).

3.7 Solitons and shock waves

Besides harmonics and chaos, nonlinearity may give rise to solitary waves, which can be induced by a pulse and shock wave. Solitons in granular crystals have been extensively studied [80, 187]. For the first type of NAM consisting of array of Helmholtz resonators, N. Sugimoto reported that properly designed resonators can enhance the dissipation of nonlinear shock acoustic waves in the near field [93]. He then studied the solitary wave in the same wave guide by solving the steady-wave solutions of nonlinear wave equation [94]. In a weakly nonlinear triatomic NAM model, M. Bukhari and O. Barry [188] showed the existence of solitary wave with hardening nonlinearity.

Mechanical metamaterials consisting of rigid units and elastic hinges can generate geometrical nonlinearity from the large rotations of the building blocks, and thus support the propagation of elastic vector solitons with three components (two translational and one rotational) [100]. They also present very rich behaviors such as compact pulses (akin to sound bullets) and separation of the pulses into different solitary modes [189]. These systems' wave dynamics in the continuum limit can be described by nonlinear Klein–Gordon equations, which gives wave solutions for conical waves [190]. They can also be modeled by the nonlinearly coupled Schrödinger equation [191]. Modulation instabilities appear under some particular parameter values [192], leading to rogue waves (a kind of wave with very large amplitude) [193]. Rogue waves are strongly influenced by variations in the nonlinearity, dispersion, and diffraction terms.

At present, solitons in 1D and 2D nonlinear periodic structures have been extensively examined from physics perspective, in terms of clear propagation properties and mechanisms. However, existing studies rarely relate solitons to the widely desired

shock wave dissipation and protection, which depends on beating, fundamental resonance, high- and sub-harmonic resonance [174, 194], etc. As shown by several studies [147, 195–197], inclusion of self-adaptive bandgaps, local resonances and large deformation in NAMs can accelerate the dissipation speed and improve the amount of shock wave energy. Therefore, future investigations are needed to clarify the properties, efficiency and mechanisms of shock wave attenuation in diverse NAMs, providing guidance for engineering designs.

4 Vibration and sound attenuation of nonlinear elastic metamaterials

Acoustic metamaterials have demonstrated remarkable performance in low-frequency vibration suppression, noise insulation, and sound absorption [11, 198, 199]. These performances in linear acoustic metamaterials mostly rely on local resonance [200–204]. However, local resonance is narrow-band. The effective bandwidth can be evaluated by $\gamma = f_{\text{cut}}/f_{\text{st}} - 1$, where f_{cut} and f_{st} are the cutoff and starting frequencies of the effective band. According to Eq. (1), $\gamma = \sqrt{1 + m_r/m_0} - 1$ for linear local resonance, e.g., $\gamma = 0.22$ for $m_r/m_0 = 0.5$.

As reviewed in Sect. 3, NAMs offer broadband mechanisms to obtain enhanced capability for vibration and sound attenuation [205]. For example, the self-broadening bandgap can expand the total bandgap region by eight times relative to the linear bandgap [27]. The chaotic band can realize low-frequency and broadband effects in theory [22]. There are also new mechanisms being revealed for broadband sound attenuation. Representative advances are reviewed hereafter.

4.1 Low-frequency and broadband vibration reduction

Based on the theoretical finding of chaotic band, experiments on the interesting design of strongly nonlinear NAM beam and plate demonstrated ultra-low and ultra-broadband vibration mitigation effect [23]. As shown in Fig. 10, relative to the narrow linear bandgap near 230 Hz, the vibration of the NAM in 30–1200 Hz is reduced by 20 dB without any artificial

damping element. The normalized bandwidth ($f_{\text{cutoff}}/f_{\text{start}}-1$) of vibration reduction band is expanded by two orders of magnitude, from 0.56 to 32. From the design perspective, the achieved broadband feature is attributed to the nonlinear coupling among multiple local resonances, and the nonlinear collision-friction damping. The essential mechanisms are the superposition effect of bandgaps, output saturation of nonlinear resonances, efficient energy pumping due to high-order harmonics and chaos, and modulation of nonlinear resonance modal amplitudes and shapes. These mechanisms and diverse wave behaviors are inter-related and occur concurrently, collectively attributed to the ultra-low and broadband features [89].

Via evaluating the influences of different parameters on the vibration reduction enabled by the chaotic band, Sheng et al. [90] found that the order of impact from the greatest to the smallest is as follows: frequency distance between bridging-coupling local resonance, nonlinear stiffness coefficient or incident amplitude, stiffness of primary beam, attached mass ratio. This confirms the imposing effect of bridging coupling [108] and insensitivity of attached mass ratio [21]. Thus, one can optimize the design to realize broadband vibration reduction with small attached mass [90]. For the high-stiffness honeycomb sandwich

plate, all resonances below 1000 Hz can be reduced by 20 dB with 17% attached mass [91].

A combinational design of linear and nonlinear metamaterials can offer both bandgaps and chaotic bands, thus improving the robustness, efficiency and bandwidth for wave suppression [206]. Moreover, combining vibro-impact motion with damping can generate robust hyper-damping effect to improve the vibration reduction effect of NAMs [185]. Nonlinear resonances and nonstationary responses of a NAM beam with cubic resonators were also analyzed by Casalotti et al. [207].

More NAMs have been designed for vibration reduction. Zhao et al. [208] proposed a nonlinear metastructure with periodically distributed bi-linear oscillators for broadband vibration suppression. Xu et al. [209, 210] studied the dissipative elastic metamaterials rotor with geometrical and damping nonlinearity. They showed that linear damping has a better capacity in reducing the vibration amplitude than nonlinear damping due to the energy dissipation near the resonance region. Wang et al. [211] proposed a nonlinear metamaterial beam with inverse nonlinearity, in which an array of piezoelectric patches was installed on a beam with shunted digital nonlinear inductor-capacitor circuits. The setting ensures an inverse nonlinear relationship between the stress and

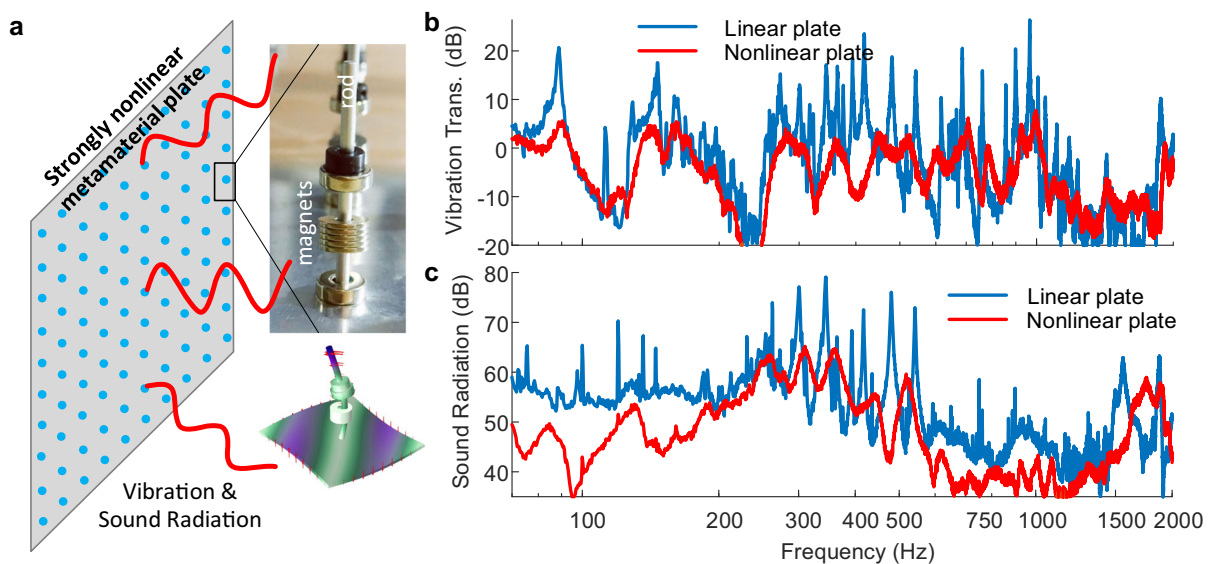


Fig. 10 Broadband reduction of vibration and sound radiation in a NAM plate [23, 89]. **a** NAM plate and its metacell. **b** Experimental vibration transmission of linear and nonlinear

metamaterial plate. **c** Experimental normalized sound radiation of linear and nonlinear metamaterial plate. Results demonstrate a great reduction of vibration and sound radiation

strain of the metamaterial. Therefore, its vibration attenuation under small-amplitude excitations is larger than that with relatively large amplitude excitations. A piezoelectric metamaterial beam with nonlinear SSDI (synchronized switching damping on inductor) dual-connected electronic networks were reported in Ref. [212].

Apart from vibration control, Tian et al. [213] and Sheng et al. [214, 215] extended the study of NAM to aeroelastic fluid–structure interaction and flow-induced vibration reduction for plates or cantilever wings in high-speed flow (Fig. 11a). NAM design may offer efficient post-flutter vibration reduction [213]. However, the critical flutter speed of a NAM plate could only be delayed by 2–5% (Fig. 11c) [214]. Nevertheless, the NAM methods could greatly reduce the broadband pre-flutter vibration with < 10% mass ratio with prior robustness (Fig. 11d,e). Furthermore, the properly designed NAM can accommodate to the varying and high temperature, which greatly reduces both wing's stiffness and resonators' frequency [215]. Besides the damping effect from high-speed flow, the reduction was also associated with bandgap and chaotic effects.

Bistable oscillator can lead to robust and highly efficient targeted energy transfer to dissipate the shock energy, owing to its unique sub-harmonic resonance capture and sub-harmonic beating along with 1:1 fundamental resonance capture and beating [194]. Recently, Hu et al. [216] proposed a 2D metamaterial aircraft wing model consisting of bi-stable nonlinear resonators, and investigated its transient fluid–structure interaction shock vibration based on an equivalent model. As shown in Fig. 11b, the bi-stable metamaterial can quickly and efficiently dissipate the transient vibration energy of the wing, outperforming the linear and mono-stable nonlinear counterparts. An energy dissipation rate of over 75% was achievable with an added mass ratio of 4–8%. The sub-harmonic nonlinear beatings and sub-harmonic resonance capture, such as 1:2 or 2:3 resonances between multiple modes, underpin the essential mechanisms for achieved performance.

The above review indicates that NAM structures can offer extraordinary and robust low-frequency and broadband vibration reduction effects, offering a promising solution for engineering applications. The mechanisms underpinning existing designs are clarified. Specially, the reported models are often high-

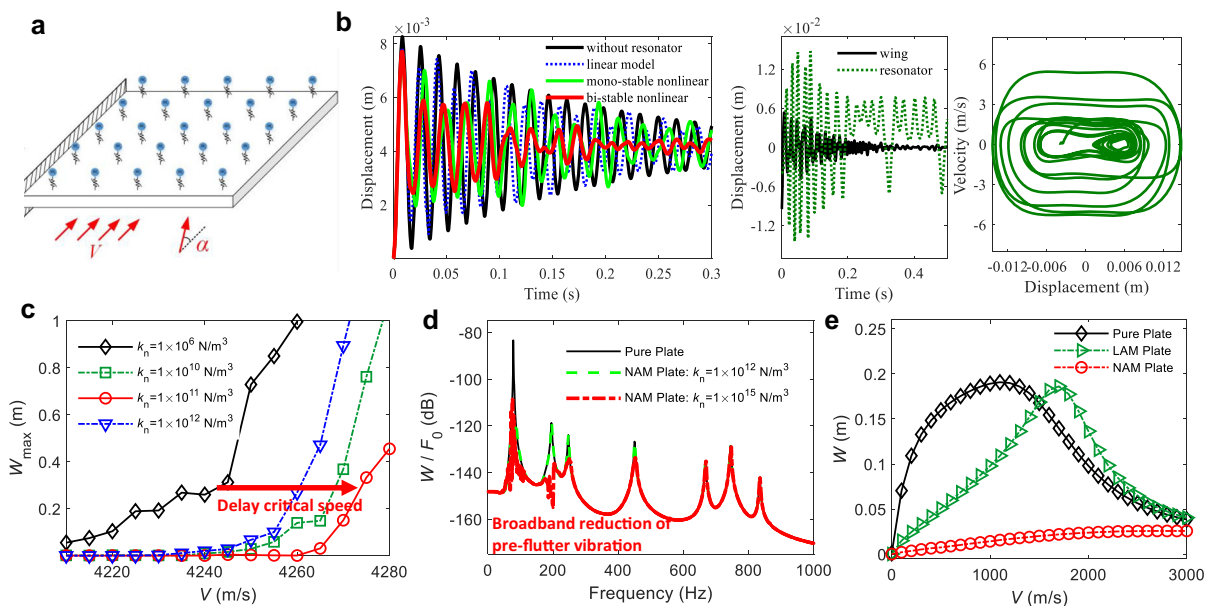


Fig. 11 Fluid–structure coupling attenuation of wing models. **a** The model of a cantilever beam in flow. **b** Reduction of transient fluid shock of a NAM wing with embedded bistable oscillators [216]. **c–e** Results of NAM wing with embedded mono-stable oscillators [214, 215]. **c** Vibration

amplitude versus flow speed, showing the delay of critical speed. **d** Broadband reduction of pre-flutter vibration. **e** Pre-flutter vibration amplitude versus flow speed, showing the efficient of NAM design

dimensional systems which may contain non-smooth nonlinearity. Numerical integration, harmonic balance, continuation, experimental signal processing form a cluster of tools to study the bifurcations, harmonics, chaos and energy dissipation in complex NAM systems. This topic can further be extended in several directions. It remains unclear if the interaction between resonances, sub-harmonic bandgaps, nonreciprocity, solitons can help improve the vibration reduction, shock energy absorption and energy harvesting. New designs and experimental demonstrations are expected in the future.

4.2 Sound radiation, absorption and insulation

As shown in Fig. 10, broadband vibration reduction of a NAM plate results in a sound radiation reduction of 10–15 dB relative to the linear metamaterial plate [89]. The NAM plate radiates sound with many high-order harmonics that lead to efficient energy transfer. Zhang et al. [98] analytically and experimentally studied the nonlinear wave scattering in a 1D air-filled waveguide periodically side-loaded by holes by considering nonlinear acoustic effects. In the low-frequency range, an enhancement was observed in absorption coefficient with increasing incident sound level owing to the nonlinear loss, as shown in Fig. 12a. However, in an acoustic absorber with several resonances, the theoretical and experimental studies established by Brooke et al. [99] showed that the sound absorption coefficient at the resonant peaks decreases when increasing the sound pressure, as shown in Fig. 12b.

To investigate the nonlinear sound insulation, Fang et al. [31] recently established a basic 1D model, consisting of two nonlinear local resonators and elastic boundaries, to simulate the acoustic/elastic wave insulation. As shown in Fig. 12c, they found that by introducing dual-position strongly nonlinear interactions, between the primary mass and the first resonator attached on it, the bandwidth for superior wave insulation can be expanded by 2–3 times relative to the optimal linear model with the same mass. Meanwhile, the insulation valley arising from the coincident effects can also be eliminated. The mechanisms were elucidated by combining the bifurcations, stability, effective mass. The results show the possibility of breaking the mass law governing the acoustic wave insulation in linear panel structures through exploring system nonlinearity, while broadening the frequency bandwidth for effective sound insulation.

However, contrast to the great achievements made in linear metamaterials, controlling sound waves with NAMs is still in an early stage of development. Major issues are 2D and 3D reflection, refraction, transmission, absorption of elastic/sound waves inside NAMs and on the interfaces, as well as bandgap evaluation methods. Nonlinear theories to tackle these issues need to be established.

5 Summary and outlook

In this review, we outlined the developments leading from linear acoustic metamaterials, FPUT chains and granular crystals to nonlinear acoustic metamaterials

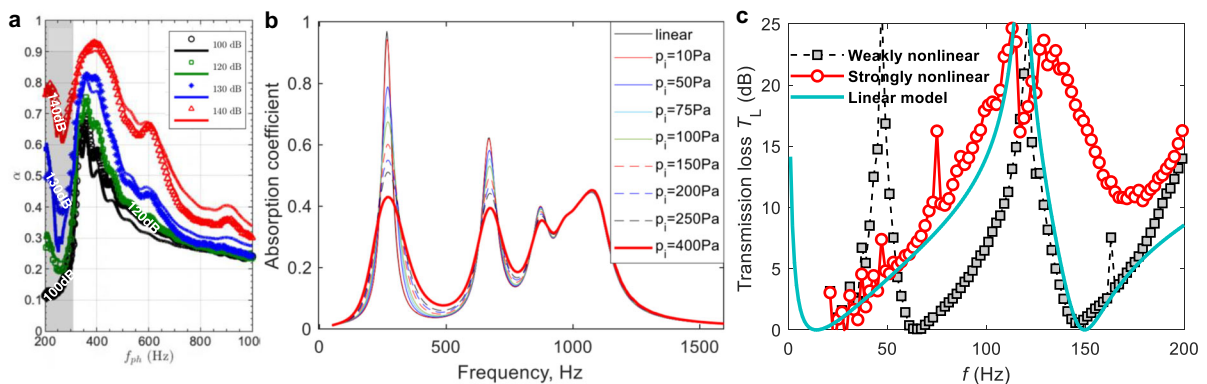


Fig. 12 Sound absorption and insulation. **a** Analytical and experimental results in Ref. [98]. **b** Results in Ref. [99]. **c** Wave transmission loss T_L of different models [31]

(NAMs). Salient properties arising from NAMs alongside underlying mechanisms and application prospect in terms of wave propagation, vibration and sound attenuation are reviewed.

NAMs have sparked a new stream of research enthusiasm, promising to revolutionize our understanding of wave behavior, unveil captivating wave phenomena, and achieve excellent engineering performance. Wave amplitude variations profoundly influence the band structure of NAMs, resulting in bandgap shifting, band degeneration and wave mode transitions that defy the stationary invariance principles observed in linear systems. Revelations of self-adaptive bands and self-broadening bandgaps challenge the traditional space–time invariance laws of linear dynamics, offering fundamental insights into wave propagation within highly nonlinear NAMs and clarifying the applicability of Bloch’s theorem. Nonlinearity in metamaterials introduces a wealth of mechanisms that disrupt the reciprocity of wave propagation, including harmonic generation, nonlinear resonance modes, amplitude-dependent bandgaps, interface effects, and chaotic responses. Extensive investigations into nonlinear wave phenomena such as frequency conversion, solitons, and breathers have provided deep insights. Moreover, chaotic band offers low-frequency and broadband phenomenon that is robustly controllable through bridging couplings between nonlinear resonant bandgaps.

NAMs designs have demonstrated unprecedented performance in vibration and sound attenuation, achieving ultra-low and ultra-broadband attenuation of structural vibrations and sound radiation through a combination of underlying mechanisms. Additionally, NAMs exhibit superior shock energy absorption compared to their linear counterparts. By replacing mono-stable nonlinear resonators with bi-stable ones, NAMs can further enhance transient energy dissipation via sub-harmonic beating and resonance, presenting promising avenues for aeroelastic vibration reduction. Preliminary research also suggests enhanced sound absorption and insulation capabilities, offering possibilities to overcome the limitations inherent in linear wave dynamics.

We discussed potential directions and challenges that should be addressed in the future, and shared views about possible avenues for solving these issues. These include efficient and accurate analysis methods, exploration of new phenomena and mechanisms, new

designs, realizations, and experimental validations. Novel wave phenomena and advanced functionality may be realized by including different types of nonlinearity in programmable mechanical metamaterials [217], phononic crystals, acoustic and topological metamaterials [218] and active control. For example, nonlinearity induces another dimension for modulating behaviors of roton-like quasiparticles [219–221]; fractional damping [222, 223] in nonlinear phononic crystals can also lead to a suitable tuning of the nonlinear bandgaps. Moreover, practical applications of NAMs are scarce at the present stage. There is a need for concerted efforts in exploring engineering applications of NAMs and developing new techniques for manipulating nonlinear waves, exemplified by the development of active control methods [224], and more recent attempts with topological designs of meta-devices for nonlinear wave manipulation, and nonlinear guided wave-based structural health monitoring of engineering materials/structures [225–229].

Acknowledgements This work is supported by the National Natural Science Foundation of China (Grant Nos. 52241103 and 52322505), Natural Science Fund of Hunan Province in China (Project No. 2023JJ10055). W.L. acknowledges the support from Project ECS 0000024 Rome Technopole, CUP B83C22002820006, National Recovery and Resilience Plan (NRRP) Mission 4 Component 2 Investment 1.5, funded by the European Union-NextGenerationEU. L.C. acknowledges the support from the Research Grants Council of Hong Kong Special Administrative Region (PolyU 152013/21E) and the Innovation and Technology Commission of the HKSAR Government to the Hong Kong Branch of National Rail Transit Electrification and Automation Engineering Technology Research Center (K-BBY1).

Author contributions X. Fang conceived the review, collated papers and wrote the draft. W. Lacarbonara and L. Cheng supplemented papers, commented, extended and revised the manuscript. All authors contributed to the study and approved the final manuscript.

Funding National Natural Science Foundation of China, 52241103, Science Fund for Distinguished Young Scholars of Hunan Province, 2023JJ10055, Project ECS 0000024 Rome Technopole, CUP B83C22002820006, European Union - NextGenerationEU, National Recovery and Resilience Plan, Research Grant Council of the Hong Kong SAR

Data availability The data that support the findings of this study are available upon reasonable request from the authors.

Declarations

Conflict of interest The authors declare that they have no conflict of interest.

Open Access This article is licensed under a Creative Commons Attribution-NonCommercial-NoDerivatives 4.0 International License, which permits any non-commercial use, sharing, distribution and reproduction in any medium or format, as long as you give appropriate credit to the original author(s) and the source, provide a link to the Creative Commons licence, and indicate if you modified the licensed material. You do not have permission under this licence to share adapted material derived from this article or parts of it. The images or other third party material in this article are included in the article's Creative Commons licence, unless indicated otherwise in a credit line to the material. If material is not included in the article's Creative Commons licence and your intended use is not permitted by statutory regulation or exceeds the permitted use, you will need to obtain permission directly from the copyright holder. To view a copy of this licence, visit <http://creativecommons.org/licenses/by-nc-nd/4.0/>.

References

1. Ford, J.: The fermi-pasta-ulam problem: paradox turns discovery. *Phys. Rep.* **213**(5), 271–310 (1992)
2. Ponno, A.: The fermi-pasta-ulam problem in the thermodynamic limit: springer Netherlands. *Math. Phys. Chem.* **182**, 431–440 (2005)
3. Berman, G.P., Izrailev, F.M.: The fermi–pasta–ulam problem: fifty years of progress. *Chaos: Int. J. Nonlinear Sci.* **15**(1), 015104 (2005)
4. Patil, G.U., Matlack, K.H.: Review of exploiting nonlinearity in phononic materials to enable nonlinear wave responses. *Acta Mech.* **233**(1), 1–46 (2022)
5. Nesterenko, V.F.: Dynamics of heterogeneous materials. Springer, New York (2001)
6. Christodoulides, D.N., Joseph, R.I.: Slow bragg solitons in nonlinear periodic structures. *Phys. Rev. Lett.* **62**, 1746 (1989)
7. Winful, H.G., Zamir, R., Feldman, S.: Modulational instability in nonlinear periodic structures: implications for gap solitons. *Appl. Phys. Lett.* **58**(10), 1001–1003 (1991)
8. Kim, E., Li, F., Chong, C., Theocharis, G., Yang, J., Kevrekidis, P.G.: Highly nonlinear wave propagation in elastic woodpile periodic structures. *Phys. Rev. Lett.* **114**(11), 118002 (2015)
9. Liu, Z., Zhang, X., Mao, Y., Zhu, Y.Y., Yang, Z., Chan, C.T., Sheng, P.: Locally resonant sonic materials. *Science* **289**(5485), 1734–1736 (2000)
10. Li, J., Chan, C.T.: Double-negative acoustic metamaterial. *Phys. Rev. E* **70**(5), 055602 (2004)
11. Ma, G., Sheng, P.: Acoustic metamaterials: from local resonances to broad horizons. *Sci. Adv.* **2**(2), e1501595 (2016)
12. Cummer, S.A., Christensen, J., Alù, A.: Controlling sound with acoustic metamaterials. *Nat. Rev. Mater.* **1**(3), 16001 (2016)
13. Ji, J.C., Luo, Q., Ye, K.: Vibration control based metamaterials and origami structures: a state-of-the-art review. *Mech. Syst. Signal Process.* **161**, 107945 (2021)
14. Brûlé, S., Enoch, S., Guenneau, S.: Emergence of seismic metamaterials: current state and future perspectives. *Phys. Lett. A* **384**(1), 126034 (2020)
15. Lapine, M., Shadrivov, I.V., Kivshar, Y.S.: Colloquium: nonlinear metamaterials. *Rev. Mod. Phys.* **86**(3), 1093–1123 (2014)
16. Li, G., Zhang, S., Zentgraf, T.: Nonlinear photonic metasurfaces. *Nat. Rev. Mater.* (2017). <https://doi.org/10.1038/natrevmats.2017.10>
17. Yang, K., Verre, R., Butet, J., Yan, C., Antosiewicz, T.J., Käll, M., Martin, O.J.F.: Wavevector-selective nonlinear plasmonic metasurfaces. *Nano Lett.* **17**(9), 5258–5263 (2017)
18. Ou, J., Plum, E., Zhang, J., Zheludev, N.I.: Giant nonlinearity of an optically reconfigurable plasmonic metamaterial. *Adv. Mater.* **28**(4), 729–733 (2016)
19. Kruk, S., et al.: Nonlinear light generation in topological nanostructures. *Nature Nanotechnol.* **14**(2), 126–130 (2018)
20. Fang, X., Wen, J., Yin, J., Yu, D.: Wave propagation in nonlinear metamaterial multi-atomic chains based on homotopy method. *AIP Adv.* **6**(12), 121706 (2016)
21. Fang, X., Wen, J., Yin, J., Yu, D., Xiao, Y.: Broadband and tunable one-dimensional strongly nonlinear acoustic metamaterials: theoretical study. *Phys. Rev. E* **94**(5), 052206 (2016)
22. Fang, X., Wen, J., Bonello, B., Yin, J., Yu, D.: Wave propagation in one-dimensional nonlinear acoustic metamaterials. *New J. Phys.* **19**(5), 053007 (2017)
23. Fang, X., Wen, J., Bonello, B., Yin, J., Yu, D.: Ultra-low and ultra-broad-band nonlinear acoustic metamaterials. *Nat. Commun.* **8**(1), 1288 (2017)
24. Khajehtourian, R., Hussein, M.I.: Dispersion characteristics of a nonlinear elastic metamaterial. *AIP Adv.* **4**(12), 124308 (2014)
25. Gong, C., Fang, X., Cheng, L.: Band degeneration and evolution in nonlinear triatomic metamaterials. *Nonlinear Dyn.* **111**(1), 97–112 (2023)
26. Silva, P.B., Leamy, M.J., Geers, M.G.D., Kouznetsova, V.G.: Emergent subharmonic band gaps in nonlinear locally resonant metamaterials induced by autoparametric resonance. *Phys. Rev. E* **99**(6), 063003 (2019)
27. Fang, X., Wen, J., Benisty, H., Yu, D.: Ultrabroad acoustic limiting in nonlinear metamaterials due to adaptive-broadening band-gap effect. *Phys. Rev. B* **101**(10), 104304 (2020)
28. Zhang, J., Romero-García, V., Theocharis, G., Richoux, O., Achilleos, V., Frantzeskakis, D.: Second-harmonic generation in membrane-type nonlinear acoustic metamaterials. *Crystals* **6**(8), 86 (2016)
29. Boechler, N., Theocharis, G., Daraio, C.: Bifurcation-based acoustic switching and rectification. *Nat. Mater.* **10**(9), 665–668 (2011)
30. Liang, B., Guo, X.S., Tu, J., Zhang, D., Cheng, J.C.: An acoustic rectifier. *Nat. Mater.* **9**(12), 989–992 (2010)

31. Fang, X., Li, T., Hu, B., Yu, M., Sheng, P., Wen, J., Cheng, L.: Breaking the mass law for broadband sound insulation through strongly nonlinear interactions. *New J. Phys.* **25**(9), 093010 (2023)
32. Weeks, R.A.: paramagnetic resonance of lattice defects in irradiated quartz. *J. Appl. Phys.* **27**(11), 1376–1381 (1956)
33. Martin, T.P.: Infrared absorption induced by a charge defect in an ionic crystal. *Phys. Rev.* **170**, 779 (1968)
34. Kushwaha, M.S., Halevi, P., Dobrzynski, L., Djafari-Rouhani, B.: Acoustic band structure of periodic elastic composites. *Phys. Rev. Lett.* **71**(13), 2022–2025 (1993)
35. Martínez-Sala, R., Sancho, J., Sánchez, J.V., Gómez, V., Llinares, J., Meseguer, F.: Sound attenuation by sculpture. *Nature* **378**(6554), 241–241 (1995)
36. Liu, Z., Chan, C.T., Sheng, P.: Analytic model of phononic crystals with local resonances. *Phys. Rev. B* **71**(1), 014103 (2005)
37. Lee, S.H., Wright, O.B.: Origin of negative density and modulus in acoustic metamaterials. *Phys. Rev. B* **93**(2), 024302 (2016)
38. Fang, N., Xi, D., Xu, J., Ambati, M., Srituravanich, W., Sun, C., Zhang, X.: Ultrasonic metamaterials with negative modulus. *Nat. Mater.* **5**(6), 452–456 (2006)
39. Li, Y., Liang, B., Gu, Z.M., Zou, X.Y., Cheng, J.C.: Reflected wavefront manipulation based on ultrathin planar acoustic metasurfaces. *Sci. Rep.* **3**(1), 2546 (2013)
40. Qu, S., Sheng, P.: Microwave and acoustic absorption metamaterials. *Phys. Rev. Appl.* **17**(4), 047001 (2022)
41. Ma, G., Yang, M., Xiao, S., Yang, Z., Sheng, P.: Acoustic metasurface with hybrid resonances. *Nat. Mater.* **13**(9), 873–878 (2014)
42. Xia, B., Li, L., Liu, J., Yu, D.: Acoustic metamaterial with fractal coiling up space for sound blocking in a deep subwavelength scale. *J. Vib. Acoust.* **140**(1), 011011 (2018)
43. Kaina, N., Lemoult, F., Fink, M., Lerosey, G.: Negative refractive index and acoustic superlens from multiple scattering in single negative metamaterials. *Nature* **525**(7567), 77–81 (2015)
44. Zhou, G., Wu, J.H., Lu, K., Tian, X., Huang, W., Zhu, K.: Broadband low-frequency membrane-type acoustic metamaterials with multi-state anti-resonances. *Appl. Acoust.* **159**, 107078 (2020)
45. Wang, X., Chen, Y., Zhou, G., Chen, T., Ma, F.: Synergetic coupling large-scale plate-type acoustic metamaterial panel for broadband sound insulation. *J. Sound Vib.* **459**, 114867 (2019)
46. Wang, X., Luo, X., Zhao, H., Huang, Z.: Acoustic perfect absorption and broadband insulation achieved by double-zero metamaterials. *Appl. Phys. Lett.* **112**(2), 021901 (2018)
47. Norris, A.N.: Acoustic cloaking theory. *Proceed. R. Soc. A: Math. Phys. Eng. Sci.* **464**(2097), 2411–2434 (2008)
48. Zhang, S., Xia, C., Fang, N.: Broadband acoustic cloak for ultrasound waves. *Phys. Rev. Lett.* **106**(2), 024301 (2011)
49. Pendry, J.B., Schurig, D., Smith, D.R.: Controlling electromagnetic fields. *Science* **312**(5781), 1780–1782 (2006)
50. Norris, A.N., Shuvalov, A.L.: Elastic cloaking theory. *Wave Motion* **48**(6), 525–538 (2011)
51. Yan, W., Yan, M., Ruan, Z., Qiu, M.: Coordinate transformations make perfect invisibility cloaks with arbitrary shape. *New J. Phys.* **10**(4), 043040 (2008)
52. Chen, Y., et al.: Broadband solid cloak for underwater acoustics. *Phys. Rev. B* **95**, 180104 (2017)
53. Zhang, H.K., Chen, Y., Liu, X.N., Hu, G.K.: An asymmetric elastic metamaterial model for elastic wave cloaking. *J. Mech. Phys. Solids* **135**, 103796 (2020)
54. Yang, Z., Gao, F., Shi, X., Lin, X., Gao, Z., Chong, Y., Zhang, B.: Topological acoustics. *Phys. Rev. Lett.* **114**(11), 114301 (2015)
55. Ge, H., Yang, M., Ma, C., Lu, M., Chen, Y., Fang, N., Sheng, P.: Breaking the barriers: advances in acoustic functional materials. *Natl. Sci. Rev.* **5**(2), 159–182 (2018)
56. He, C., et al.: Acoustic topological insulator and robust one-way sound transport. *Nat. Phys.* **12**(12), 1124–1129 (2016)
57. Miniaci, M., Pal, R.K., Morvan, B., Ruzzene, M.: Experimental observation of topologically protected helical edge modes in patterned elastic plates. *Phys. Rev. X* **8**(3), 031074 (2018)
58. Wang, W., Bonello, B., Djafari-Rouhani, B., Pennec, Y.: Topological valley, pseudospin, and pseudospin-valley protected edge states in symmetric pillared phononic crystals. *Phys. Rev. B* (2019). <https://doi.org/10.1103/PhysRevB.100.140101>
59. Hasan, M.Z., Kane, C.L.: Colloquium: : topological insulators. *Rev. Mod. Phys.* **82**(4), 3045–3067 (2010)
60. Souslov, A., van Zuijden, B.C., Bartolo, D., Vitelli, V.: Topological sound in active-liquid metamaterials. *Nat. Phys.* **13**(11), 1091–1094 (2017)
61. Qi, Y., Qiu, C., Xiao, M., He, H., Ke, M., Liu, Z.: Acoustic realization of quadrupole topological insulators. *Phys. Rev. Lett.* **124**(20), 206601 (2020)
62. Wei, Q., et al.: Higher-order topological semimetal in acoustic crystals. *Nature Mater.* (2021). <https://doi.org/10.1038/s41563-021-00933-4>
63. Luo, L., Wang, H., Lin, Z., Jiang, B., Wu, Y., Li, F., Jiang, J.: Observation of a phononic higher-order Weyl semimetal. *Nature Mater.* (2021). <https://doi.org/10.1038/s41563-021-00985-6>
64. Lu, J., Qiu, C., Ye, L., Fan, X., Ke, M., Zhang, F., Liu, Z.: Observation of topological valley transport of sound in sonic crystals. *Nat. Phys.* **13**(4), 369–374 (2017)
65. He, H., et al.: Topological negative refraction of surface acoustic waves in a Weyl phononic crystal. *Nature* **560**(7716), 61–64 (2018)
66. Murer, M., Gुरुva, S.K., Formica, G., Lacarbonara, W.: A multi-bandgap metamaterial with multi-frequency resonators. *J. Compos. Mater.* **57**(4), 783–804 (2023)
67. Fermi, E., Pasta, J., Ulam, S.: Studies of nonlinear problems. In *Los Alamos Sci. Lab. Rept.*, LA-1940, (1955)
68. Babicheva, R.I., Semenov, A.S., Soboleva, E.G., Kudreyko, A.A., Zhou, K., Dmitriev, S.V.: Discrete breathers in a triangular β -Fermi-Pasta-Ulam-Tsingou lattice. *Phys. Rev. E* (2021). <https://doi.org/10.1103/PhysRevE.103.052202>
69. Onorato, M., Lvov, Y.V., Dematteis, G., Chibbaro, S.: Wave turbulence and thermalization in one-dimensional chains. *Phys. Rep.* **1040**, 1–36 (2023)

70. Chaunsali, R., Kevrekidis, P.G., Frantzeskakis, D., Theocharis, G.: Dirac solitons and topological edge states in the beta-Fermi-Pasta-Ulam-Tsingou dimer lattice. *Phys. Rev. E* **108**(5–1), 054224 (2023)
71. Feng, S., Fu, W., Zhang, Y., Zhao, H.: The anti-Fermi-Pasta-Ulam-Tsingou problem in one-dimensional diatomic lattices. *J. Stat. Mech: Theory Exp.* **2022**(5), 053104 (2022)
72. Olver, P.J., Stern, A.: Dispersive fractalisation in linear and nonlinear Fermi-Pasta-Ulam-Tsingou lattices. *Eur. J. Appl. Math.* **32**(5), 820–845 (2021)
73. Nfor, N.O., Yamgoué, S.B., Moukam Kakmeni, F.M.: Investigation of bright and dark solitons in α , β -Fermi Pasta Ulam lattice. *Chine. Phys. B* **30**(2), 020502 (2021)
74. Pankov, A.: Solitary waves on nonlocal Fermi-Pasta-Ulam lattices: Exponential localization. *Nonlinear Anal. Real World Appl.* **50**, 603–612 (2019)
75. James, G., Pelinovsky, D.: Gaussian solitary waves and compactons in Fermi-Pasta-Ulam lattices with Hertzian potentials. *Proceed. Royal Soc. A: Math. Phys. Eng. Sci.* **470**(2165), 20130462 (2014)
76. Simadji Ngamou, C., Ndjomatchoua, F.T., Mekontchou Foudjio, M., Gninzanlong, C.L., Tchawoua, C.: Supra-transmission phenomenon in a Fermi-Pasta-Ulam diatomic lattice. *Phys. Rev. E* **108**(5–1), 054216–054216 (2023)
77. Kim, E., Yang, J.: Review: wave propagation in granular metamaterials. *Function. Compos. Struct.* **1**(1), 012002 (2019)
78. Chong, C., Porter, M.A., Kevrekidis, P.G., Daraio, C.: Nonlinear coherent structures in granular crystals. *J. Phys. Condens. Matter* **29**(41), 413003 (2017)
79. Nesterenko, V.F.: Waves in strongly nonlinear discrete systems. *Philos. Trans. A Math. Phys. Eng. Sci.* **376**(2127), 20170130 (2018)
80. Daraio, C., Nesterenko, V.F., Herbold, E.B., Jin, S.: Tunability of solitary wave properties in one-dimensional strongly nonlinear phononic crystals. *Phys. Rev. E* **73**(2), 026610 (2006)
81. Spadoni, A., Daraio, C.: Generation and control of sound bullets with a nonlinear acoustic lens. *Proc. Natl. Acad. Sci.* **107**(16), 7230–7234 (2010)
82. Nesterenko, V.F., Daraio, C., Herbold, E.B., Jin, S.: Anomalous wave reflection at the interface of two strongly nonlinear granular media. *Phys. Rev. Lett.* **95**(15), 158702 (2005)
83. Boechler, N., Theocharis, G., Job, S., Kevrekidis, P.G., Porter, M.A., Daraio, C.: Discrete breathers in one-dimensional diatomic granular crystals. *Phys. Rev. Lett.* **104**(24), 244302 (2010)
84. Chong, C., Kevrekidis, P.G., Theocharis, G., Daraio, C.: Dark breathers in granular crystals. *Phys. Rev. E* **87**(4), 042202 (2013)
85. Gohman, P.A., Bambakidis, G., Spry, R.J.: Theoretical intensity-dependent response of nonlinear periodic structures. *J. Appl. Phys.* **67**(1), 40–44 (1990)
86. Martijn de Sterke, C., Sipe, J.E.: Switching dynamics of finite periodic nonlinear media: a numerical study. *Phys. Rev. A* **42**(5), 2858–2869 (1990)
87. de Sterke, C.M.: Stability analysis of nonlinear periodic media. *Phys. Rev. A* **45**(11), 8252–8258 (1992)
88. Scalora, M., Bloemer, M.J., Manka, A.S., Dowling, J.P., Bowden, C.M., Viswanathan, R., Haus, J.W.: Pulsed second-harmonic generation in nonlinear, one-dimensional, periodic structures. *Phys. Rev. A* **56**(4), 3166–3174 (1997)
89. Fang, X., Sheng, P., Wen, J., Chen, W., Cheng, L.: A nonlinear metamaterial plate for suppressing vibration and sound radiation. *Int. J. Mech. Sci.* **228**, 107473 (2022)
90. Sheng, P., Fang, X., Wen, J., Yu, D.: Vibration properties and optimized design of a nonlinear acoustic metamaterial beam. *J. Sound Vib.* **492**, 115739 (2021)
91. Sheng, P., Fang, X., Dai, L., Yu, D., Wen, J.: Synthetical vibration reduction of the nonlinear acoustic metamaterial honeycomb sandwich plate. *Mech. Syst. Signal Process.* **185**, 109774 (2023)
92. Cha, J., Daraio, C.: Electrical tuning of elastic wave propagation in nanomechanical lattices at MHz frequencies. *Nature Nanotechnol.* **13**(11), 1016–1020 (2018)
93. Sugimoto, N.: Propagation of nonlinear acoustic waves in a tunnel with an array of Helmholtz resonators. *J. Fluid Mech.* **244**(1), 55–78 (1992)
94. Sugimoto, N.: Acoustic solitary waves in a tunnel with an array of Helmholtz resonators. *J. Acoust. Soc. Am.* **99**(4), 1971–1976 (1996)
95. Bradley, C.E.: Time harmonic acoustic Bloch wave propagation in periodic waveguides. Part I. Theory. *J. Acoust. Soc. Am.* **96**(3), 1844–1853 (1994)
96. Bradley, C.E.: Time harmonic acoustic Bloch wave propagation in periodic waveguides. Part II. Experiment. *J. Acoust. Soc. Am.* **96**(3), 1854–1862 (1994)
97. Bradley, C.E.: Time-harmonic acoustic Bloch wave propagation in periodic waveguides. Part III. Nonlinear effects. *J. Acoust. Soc. Am.* **98**(5), 2735–2744 (1995)
98. Zhang, J., Romero-García, V., Theocharis, G., Richoux, O., Achilleos, V., Frantzeskakis, D.J.: High-amplitude sound propagation in acoustic transmission-line metamaterial. *Appl. Phys. Lett.* **118**(10), 104102 (2021)
99. Brooke, D.C., Umnova, O., Leclaire, P., Dupont, T.: Acoustic metamaterial for low frequency sound absorption in linear and nonlinear regimes. *J. Sound Vib.* **485**, 115585 (2020)
100. Deng, B., Wang, P., He, Q., Tournat, V., Bertoldi, K.: Metamaterials with amplitude gaps for elastic solitons. *Nat. Commun.* **9**(1), 3410 (2018)
101. Shen, Y., Lacarbonara, W.: Nonlinearity enhanced wave bandgaps in metamaterial honeycombs embedding spider web-like resonators. *J. Sound Vib.* **562**, 117821 (2023)
102. Silverberg, J.L., et al.: Origami structures with a critical transition to bistability arising from hidden degrees of freedom. *Nat. Mater.* **14**(4), 389–393 (2015)
103. Overvelde, J.T.B., Weaver, J.C., Hoberman, C., Bertoldi, K.: Rational design of reconfigurable prismatic architected materials. *Nature* **541**(7637), 347–352 (2017)
104. Xiu, H., et al.: Topological transformability and reprogrammability of multistable mechanical metamaterials. *Proceed. Nation. Acad. Sci.—PNAS* **119**(52), e2211725119–e2211725119 (2022)
105. Mofatteh, H., Shahryari, B., Mirabolghasemi, A., Seyedkanani, A., Shirzadkhani, R., Desharnais, G., Akbarzadeh, A.: Programming multistable metamaterials to discover latent functionalities. *Adv. Sci.* (2022). <https://doi.org/10.1002/adv.202202883>

106. Ma, H., Wang, K., Zhao, H., Mu, R., Yan, B.: A reusable metastructure for tri-directional energy dissipation. *Int. J. Mech. Sci.* **214**, 106870 (2022)
107. Fan, H., Tian, Y., Yang, L., Hu, D., Liu, P.: Multistable mechanical metamaterials with highly tunable strength and energy absorption performance. *Mech. Adv. Mater. Struct.* **29**(11), 1637–1649 (2022)
108. Fang, X., Wen, J., Yu, D., Yin, J.: Bridging-coupling band gaps in nonlinear acoustic metamaterials. *Phys. Rev. Appl.* **10**(5), 054049 (2018)
109. Narisetti, R.K., Leamy, M.J., Ruzzene, M.: A perturbation approach for predicting wave propagation in one-dimensional nonlinear periodic structures. *J. Vibrat. Acoust. DOI* **10**(115/1), 4000775 (2010)
110. Shen, Y., Lacarbonara, W.: Nonlinear dispersion properties of metamaterial beams hosting nonlinear resonators and stop band optimization. *Mech. Syst. Signal Process.* **187**, 109920 (2023)
111. Narisetti, R.K., Ruzzene, M., Leamy, M.J.: Study of wave propagation in strongly nonlinear periodic lattices using a harmonic balance approach. *Wave Motion* **49**(2), 394–410 (2012)
112. Narisetti, R.K., Ruzzene, M., Leamy, M.J.: A perturbation approach for analyzing dispersion and group velocities in two-dimensional nonlinear periodic lattices. *J. Vibrat. Acoust.* **133**(6), 061020 (2011)
113. Zhao, C., Zhang, K., Zhao, P., Deng, Z.: Elastic wave propagation in nonlinear two-dimensional acoustic metamaterials. *Nonlinear Dyn.* **108**(2), 743–763 (2022)
114. Manktelow, K.L., Leamy, M.J., Ruzzene, M.: Weakly nonlinear wave interactions in multi-degree of freedom periodic structures. *Wave Motion* **51**(6), 886–904 (2014)
115. Fortunati, A., Bacigalupo, A., Lepidi, M., Arena, A., Lacarbonara, W.: Nonlinear wave propagation in locally dissipative metamaterials via Hamiltonian perturbation approach. *Nonlinear Dyn.* **108**(2), 765–787 (2022)
116. Fortunati, A., Arena, A., Lepidi, M., Bacigalupo, A., Lacarbonara, W.: Free propagation of resonant waves in nonlinear dissipative metamaterials. *Proceed. Royal Soc. A: Math. Phys. Eng. Sci.* (2024). <https://doi.org/10.1098/rspa.2023.0759>
117. Narisetti, R.K.: Wave propagation in nonlinear periodic structures. Georgia Institute of Technology, Atlanta (2010)
118. Fang, X., Wen, J., Yu, D., Huang, G., Yin, J.: Wave propagation in a nonlinear acoustic metamaterial beam considering third harmonic generation. *New J. Phys.* **20**(12), 123028 (2018)
119. Zhou, W.J., Li, X.P., Wang, Y.S., Chen, W.Q., Huang, G.L.: Spectro-spatial analysis of wave packet propagation in nonlinear acoustic metamaterials. *J. Sound Vib.* **413**, 250–269 (2018)
120. Xu, Y., Nesterenko, V.F.: Propagation of short stress pulses in discrete strongly nonlinear tunable metamaterials. *Philos. Trans. Royal Soc. A: Math., Phys. Eng. Sci.* **372**(2023), 20130186 (2014)
121. Allein, F., Tournat, V., Gusev, V.E., Theocharis, G.: Tunable magneto-granular phononic crystals. *Appl. Phys. Lett.* **108**(16), 161903 (2016)
122. Allein, F., Tournat, V., Gusev, V., Theocharis, G.: Linear and nonlinear elastic waves in magnetogranular chains. *Phys. Rev. Appl.* **13**(2), 415401 (2020)
123. Bae, M.H., Oh, J.H.: Amplitude-induced bandgap: new type of bandgap for nonlinear elastic metamaterials. *J. Mech. Phys. Solids* **139**, 103930 (2020)
124. Liang, S., Liu, J., Lai, Y., Liu, X.: Nonlinear wave propagation in acoustic metamaterials with bilinear nonlinearity. *Chin. Phys. B* **32**(4), 44301–44463 (2023)
125. Cveticanin, L., Zukovic, M., Cveticanin, D.: Influence of nonlinear subunits on the resonance frequency band gaps of acoustic metamaterial. *Nonlinear Dyn.* **93**(3), 1341–1351 (2018)
126. Cveticanin, L., Zukovic, M.: Negative effective mass in acoustic metamaterial with nonlinear mass-in-mass subsystems. *Commun. Nonlinear Sci. Numer. Simul.* **51**, 89–104 (2017)
127. Gantounis, G., Serra-Garcia, M., Homma, K., Mendoza, J.M., Daraio, C.: Granular metamaterials for vibration mitigation. *J. Appl. Phys.* **114**(9), 093514 (2013)
128. Liu, M., Xia, B.: Research on new wave behavior and mechanisms in nonlinear diatomic acoustic metamaterials with linear damping. *Nonlinear Dyn.* **112**(1), 403–417 (2024)
129. Liu, M., Zhou, F.: Spectro-spatial analysis of nonlinear wave propagation behaviors in damped acoustic metamaterial systems. *J. Vib. Eng. Technol.* **12**(1), 53–65 (2024)
130. Jiao, W., Gonella, S.: Doubly nonlinear waveguides with self-switching functionality selection capabilities. *Phys. Rev. E* **99**(4), 042206 (2019)
131. Higashiyama, N., Nakatani, A.: Nonlinear dynamics of a model of acoustic metamaterials with local resonators. *Nonlinear Theory Appl. IEICE* **8**(2), 129–145 (2017)
132. Settimi, V., Lepidi, M., Bacigalupo, A.: Nonlinear dispersion properties of one-dimensional mechanical metamaterials with inertia amplification. *Int. J. Mech. Sci.* **201**, 106461 (2021)
133. Madhamshetty, K., Manimala, J.M.: Extraordinary wave manipulation characteristics of nonlinear inertant acoustic metamaterials. *J. Franklin Inst.* **356**(14), 7731–7753 (2019)
134. Bae, M.H., Oh, J.H.: Nonlinear elastic metamaterial for tunable bandgap at quasi-static frequency. *Mech. Syst. Signal Process.* **170**, 108832 (2022)
135. Richoux, O., Tournat, V., Le Van Suu, T.: Acoustic wave dispersion in a one-dimensional lattice of nonlinear resonant scatterers. *Phys. Rev. E* **75**(2), 026615 (2007)
136. Li, Y., Lan, J., Li, B., Liu, X., Zhang, J.: Nonlinear effects in an acoustic metamaterial with simultaneous negative modulus and density. *J. Appl. Phys.* **120**(14), 145105 (2016)
137. Lan, J., Li, Y., Yu, H., Li, B., Liu, X.: Nonlinear effects in acoustic metamaterial based on a cylindrical pipe with ordered Helmholtz resonators. *Phys. Lett. A* **381**(13), 1111–1117 (2017)
138. Bilal, O.R., Foehr, A., Daraio, C.: Reprogrammable phononic metasurfaces. *Adv. Mater.* (2017). <https://doi.org/10.1002/adma.201700628>
139. Lou, J., Fan, H., Zhang, A., Du, J.: Attenuation of Rayleigh waves by a nonlinear metamaterial with serial-connected resonators. *Acta Mech.* **234**(10), 4963–4976 (2023)
140. Kulkarni, P.P., Manimala, J.M.: Realizing passive direction-bias for mechanical wave propagation using a

- nonlinear metamaterial. *Acta Mech.* **230**(7), 2521–2537 (2019)
141. Lepidi, M., Bacigalupo, A.: Wave propagation properties of one-dimensional acoustic metamaterials with nonlinear diatomic microstructure. *Nonlinear Dyn.* **98**(4), 2711–2735 (2019)
 142. Nadkarni, N., Daraio, C., Kochmann, D.M.: Dynamics of periodic mechanical structures containing bistable elastic elements: from elastic to solitary wave propagation. *Phys. Rev. E* **90**(2), 023204 (2014)
 143. Frazier, M.J., Kochmann, D.M.: Band gap transmission in periodic bistable mechanical systems. *J. Sound Vib.* **388**, 315–326 (2017)
 144. Bernard, B.P., Mazzoleni, M.J., Garraud, N., Arnold, D.P., Mann, B.P.: Experimental investigation of bifurcation induced bandgap reconfiguration. *J. Appl. Phys.* **116**(8), 084904 (2014)
 145. Meaud, J., Che, K.: Tuning elastic wave propagation in multistable architected materials. *Int. J. Solids Struct.* **122–123**, 69–80 (2017)
 146. Wang, J., Liu, X., Yang, Q., Tao, R., Li, Y., Ma, L.: A novel programmable composite metamaterial with tunable Poisson's ratio and bandgap based on multi-stable switching. *Compos. Sci. Technol.* **219**, 109245 (2022)
 147. Liu, E., Fang, X., Wen, J.: Harmonic and shock wave propagation in bistable periodic structure: regularity, randomness, and tunability. *J. Vib. Control* **28**(21–22), 3332–3343 (2022)
 148. Zhang, S., Lou, J., Fan, H., Du, J.: A nonlinear acoustic metamaterial beam with tunable flexural wave band gaps. *Eng. Struct.* **276**, 115379 (2023)
 149. Jalas, D., et al.: What is—and what is not—an optical isolator. *Nat. Photonics* **7**(8), 579–582 (2013)
 150. Nassar, H., et al.: Nonreciprocity in acoustic and elastic materials. *Nat. Rev. Mater.* **5**(9), 667–685 (2020)
 151. Walker, E., et al.: Nonreciprocal linear transmission of sound in a viscous environment with Broken P symmetry. *Phys. Rev. Lett.* **120**(20), 204501 (2018)
 152. Nassar, H., Chen, H., Norris, A.N., Haberman, M.R., Huang, G.L.: Non-reciprocal wave propagation in modulated elastic metamaterials. *Proceed. Royal Soc. A: Math. Phys. Eng. Sci.* **473**(2202), 20170188 (2017)
 153. Trainiti, G., Ruzzene, M.: Non-reciprocal elastic wave propagation in spatiotemporal periodic structures. *New J. Phys.* **18**(8), 083047 (2016)
 154. Deymier, P.A., Gole, V., Lucas, P., Vasseur, J.O., Runge, K.: Tailoring phonon band structures with broken symmetry by shaping spatiotemporal modulations of stiffness in a one-dimensional elastic waveguide. *Phys. Rev. B* **96**(6), 064304 (2017)
 155. Yi, K., Karkar, S., Collet, M.: One-way energy insulation using time-space modulated structures. *J. Sound Vib.* **429**, 162–175 (2018)
 156. Huang, J., Zhou, X.: A time-varying mass metamaterial for non-reciprocal wave propagation. *Int. J. Solids Struct.* **164**, 25–36 (2019)
 157. Chen, Y., Li, X., Nassar, H., Norris, A.N., Daraio, C., Huang, G.: Nonreciprocal wave propagation in a continuum-based metamaterial with space-time modulated resonators. *Phys. Rev. Appl.* **11**(6), 064052 (2019)
 158. Fang, X., Wen, J., Cheng, L., Li, B.: Bidirectional elastic diode with frequency-preserved nonreciprocity. *Phys. Rev. Appl.* **15**(5), 054022 (2021)
 159. Grinberg, I., Vakakis, A.F., Gendelman, O.V.: Acoustic diode: wave non-reciprocity in nonlinearly coupled waveguides. *Wave Motion* **83**, 49–66 (2018)
 160. Blanchard, A., Sapsis, T.P., Vakakis, A.F.: Non-reciprocity in nonlinear elastodynamics. *J. Sound Vib.* **412**, 326–335 (2018)
 161. Lepri, S., Casati, G.: Asymmetric wave propagation in nonlinear systems. *Phys. Rev. Lett.* **106**(16), 164101 (2011)
 162. Li, B., Wang, L., Casati, G.: Thermal diode: rectification of heat flux. *Phys. Rev. Lett.* **93**, 184301 (2004)
 163. Li, N., Ren, J., Wang, L., Zhang, G., Hänggi, P., Li, B.: Colloquium: phononics: Manipulating heat flow with electronic analogs and beyond. *Rev. Mod. Phys.* **84**(3), 1045–1066 (2012)
 164. Wehmeyer, G., Yabuki, T., Monachon, C., Wu, J., Dames, C.: Thermal diodes, regulators, and switches: Physical mechanisms and potential applications. *Appl. Phys. Rev.* **4**(4), 041304 (2017)
 165. Wu, G., Long, Y., Ren, J.: Asymmetric nonlinear system is not sufficient for a nonreciprocal wave diode. *Phys. Rev. B* **97**(20), 205423 (2018)
 166. Li, Z., Yuan, B., Wang, Y., Shui, G., Zhang, C., Wang, Y.: Diode behavior and nonreciprocal transmission in nonlinear elastic wave metamaterial. *Mech. Mater.* **133**, 85–101 (2019)
 167. Li, Z., Wang, Y., Wang, Y.: Tunable nonreciprocal transmission in nonlinear elastic wave metamaterial by initial stresses. *Int. J. Solids Struct.* **182–183**, 218–235 (2020)
 168. Fu, C., Wang, B., Zhao, T., Chen, C.Q.: High efficiency and broadband acoustic diodes. *Appl. Phys. Lett.* **112**(5), 051902 (2018)
 169. Li, K., Rizzo, P.: Nonreciprocal propagation of solitary waves in granular chains with asymmetric potential barriers. *J. Sound Vib.* **365**, 15–21 (2016)
 170. Popa, B., Cummer, S.A.: Non-reciprocal and highly nonlinear active acoustic metamaterials. *Nature Commun.* **5**(1), 3398 (2014)
 171. Gliozzi, A.S., Miniaci, M., Krushynska, A.O., Morvan, B., Scalerandi, M., Pugno, N.M., Bosia, F.: Proof of concept of a frequency-preserving and time-invariant metamaterial-based nonlinear acoustic diode. *Sci. Rep.* **9**(1), 9560 (2019)
 172. Liu, C., Du, Z., Sun, Z., Gao, H., Guo, X.: Frequency-preserved acoustic diode model with high forward-power-transmission rate. *Phys. Rev. Appl.* **3**(6), 064014 (2015)
 173. Cui, J., Yang, T., Chen, L.: Frequency-preserved non-reciprocal acoustic propagation in a granular chain. *Appl. Phys. Lett.* **112**(18), 181904 (2018)
 174. Vakakis, A.F., Gendelman, O.V., Bergman, L.A., Mojaheid, A., Gzal, M.: Nonlinear targeted energy transfer: state of the art and new perspectives. *Nonlinear Dyn.* **108**(2), 711–741 (2022)
 175. Yun, Y., Miao, G.Q., Zhang, P., Huang, K., Wei, R.J.: Nonlinear acoustic wave propagating in one-dimensional layered system. *Phys. Lett. A* **343**(5), 351–358 (2005)

176. Ganesh, R., Gonella, S.: From modal mixing to tunable functional switches in nonlinear phononic crystals. *Phys. Rev. Lett.* **114**(5), 054302 (2015)
177. Fan, L., Ge, H., Zhang, S.Y., Gao, H.F., Liu, Y.H., Zhang, H.: Nonlinear acoustic fields in acoustic metamaterial based on a cylindrical pipe with periodically arranged side holes. *J. Acoust. Soc. Am.* **133**(6), 3846–3852 (2013)
178. Jeon, G.J., Oh, J.H.: Nonlinear acoustic metamaterial for efficient frequency down-conversion. *Phys. Rev. E* **103**(1–1), 012212 (2021)
179. Guo, X., Gusev, V.E., Bertoldi, K., Tournat, V.: Manipulating acoustic wave reflection by a nonlinear elastic metasurface. *J. Appl. Phys.* **123**(12), 124901 (2018)
180. Bonanomi, L., Theocharis, G., Daraio, C.: Wave propagation in granular chains with local resonances. *Phys. Rev. E* **91**(3), 033208 (2015)
181. Donahue, C.M., Anzel, P.W.J., Bonanomi, L., Keller, T.A., Daraio, C.: Experimental realization of a nonlinear acoustic lens with a tunable focus. *Appl. Phys. Lett.* **104**(1), 014103 (2014)
182. Hooeboom, C., Man, Y., Boechler, N., Theocharis, G., Kevrekidis, P.G., Kevrekidis, I.G., Daraio, C.: Hysteresis loops and multi-stability: from periodic orbits to chaotic dynamics (and back) in diatomic granular crystals. *EPL (Eur. Lett.)* **101**(4), 44003 (2013)
183. Lydon, J., Theocharis, G., Daraio, C.: Nonlinear resonances and energy transfer in finite granular chains. *Phys. Rev. E* **91**(2), 023208 (2015)
184. Banerjee, A., Calius, E.P., Das, R.: Impact based wideband nonlinear resonating metamaterial chain. *Int. J. Non-Linear Mech.* **103**, 138–144 (2018)
185. Yu, M., Fang, X., Yu, D., Wen, J., Cheng, L.: Collision enhanced hyper-damping in nonlinear elastic metamaterial. *Chin. Phys. B* **31**(6), 064303 (2022)
186. Beli, D., Ruzzene, M., De Marqui, J.C.: Bridging-coupling phenomenon in linear elastic metamaterials by exploiting locally resonant metachain isomers. *Phys. Rev. Appl.* **14**(3), 034032 (2020)
187. Liu, Z., Wang, Y., Huang, G.: Solitary waves in a granular chain of elastic spheres: multiple solitary solutions and their stabilities. *Phys. Rev. E* **99**(6), 062904 (2019)
188. Bukhari, M., Barry, O.: Spectro-spatial analyses of a nonlinear metamaterial with multiple nonlinear local resonators. *Nonlinear Dyn.* **99**(2), 1539–1560 (2020)
189. Deng, B., Mo, C., Tournat, V., Bertoldi, K., Raney, J.R.: Focusing and mode separation of elastic vector solitons in a 2D soft mechanical metamaterial. *Phys. Rev. Lett.* (2019). <https://doi.org/10.1103/PhysRevLett.123.024101>
190. Deng, B., Li, J., Tournat, V., Purohit, P.K., Bertoldi, K.: Dynamics of mechanical metamaterials: a framework to connect phonons, nonlinear periodic waves and solitons. *J. Mech. Phys. Solids* **147**, 104233 (2021)
191. Demiquel, A., Achilleos, V., Theocharis, G., Tournat, V.: Modulation instability in nonlinear flexible mechanical metamaterials. *Phys. Rev. E* **107**(5–1), 054212 (2023)
192. Houwe, A., Abbagari, S., Akinyemi, L., Inc, M., Doka, S.Y.: Modulation instability in nonlinear acoustic metamaterials with coupling coefficients. *Eur. Phys. J. Plus* (2023). <https://doi.org/10.1140/epjp/s13360-023-04195-8>
193. Justin, M., et al.: Rogue waves as modulational instability result in one-dimensional nonlinear triatomic acoustic metamaterials. *Wave Motion* **123**, 103224 (2023)
194. Fang, X., Wen, J., Yin, J., Yu, D.: Highly efficient continuous bistable nonlinear energy sink composed of a cantilever beam with partial constrained layer damping. *Nonlinear Dyn.* **87**(4), 2677–2695 (2017)
195. Hu, B., Fang, X., Cheng, L., Wen, J., Yu, D.: Attenuation of impact waves in a nonlinear acoustic metamaterial beam. *Nonlinear Dyn.* **111**(17), 15801–15816 (2023)
196. Mehreganian, N., Fallah, A.S., Sareh, P.: Impact response of negative stiffness curved-beam-architected metastructures. *Int. J. Solids Struct.* **279**, 112389 (2023)
197. Zhao, A., et al.: Evaluation of shock migration performance for a multi-stable mechanical metamaterial. *Compos. Struct.* **321**, 117312 (2023)
198. Henneberg, J., Gomez Nieto, J.S., Sepahvand, K., Gerlach, A., Cebulla, H., Marburg, S.: Periodically arranged acoustic metamaterial in industrial applications: the need for uncertainty quantification. *Appl. Acoust.* **157**, 107026 (2020)
199. Li, T., Fang, X., Yin, J., Wang, Y., Wang, S., Wen, J.: Integrated adjustable acoustic metacage for multi-frequency noise reduction. *Appl. Acoust.* **217**, 109841 (2024)
200. Li, Y., Yan, S., Li, H.: Wave propagation of 2D elastic metamaterial with rotating squares and hinges. *Int. J. Mech. Sci.* **217**, 107037 (2022)
201. Lin, Q., Zhou, J., Wang, K., Xu, D., Wen, G., Wang, Q., Cai, C.: Low-frequency locally resonant band gap of the two-dimensional quasi-zero-stiffness metamaterials. *Int. J. Mech. Sci.* **222**, 107230 (2022)
202. Guo, Z., Hu, G., Sorokin, V., Tang, L., Yang, X., Zhang, J.: Low-frequency flexural wave attenuation in metamaterial sandwich beam with hourglass lattice truss core. *Wave Motion* **104**, 102750 (2021)
203. Kumar, N., Pal, S.: Unraveling interactions of resonances for tunable low frequency bandgap in multiphase metamaterials under applied deformation. *Int. J. Solids Struct.* **212**, 169–201 (2021)
204. Wu, X., Wen, Z., Jin, Y., Rabczuk, T., Zhuang, X., Djafari-Rouhani, B.: Broadband Rayleigh wave attenuation by gradient metamaterials. *Int. J. Mech. Sci.* **205**, 106592 (2021)
205. Fiore, S., Finocchio, G., Zivieri, R., Chiappini, M., Garosci, F.: Wave amplitude decay driven by anharmonic potential in nonlinear mass-in-mass systems. *Appl. Phys. Lett.* **117**(12), 124101 (2020)
206. Yu, M., Fang, X., Yu, D.: Combinational design of linear and nonlinear elastic metamaterials. *Int. J. Mech. Sci.* **199**, 106422 (2021)
207. Casalotti, A., El-Borgi, S., Lacarbonara, W.: Metamaterial beam with embedded nonlinear vibration absorbers. *Int. J. Non-Linear Mech.* **98**, 32–42 (2018)
208. Zhao, T., Yang, Z., Tian, W.: Tunable nonlinear metastructure with periodic bi-linear oscillators for broadband vibration suppression. *Thin-Walled Struct.* **191**, 110975 (2023)
209. Xu, Q., Wang, J., Lv, Y., Yao, H., Wen, B.: Vibration characteristics of linear and nonlinear dissipative elastic metamaterials rotor with geometrical nonlinearity. *Int. J. Non-Linear Mech.* **157**, 104543 (2023)

210. Xu, Q., Lv, Y., Liu, Z., Yao, H., Wen, B.: Vibration characteristics of multi-acoustic metamaterials rotor with geometrical nonlinearity. *Nonlinear Dyn.* **111**(14), 12817–12833 (2023)
211. Zhang, X., Yu, H., He, Z., Huang, G., Chen, Y., Wang, G.: A metamaterial beam with inverse nonlinearity for broadband micro-vibration attenuation. *Mech. Syst. Signal Process.* **159**, 107826 (2021)
212. Bao, B., Lallart, M., Guyomar, D.: Manipulating elastic waves through piezoelectric metamaterial with nonlinear electrical switched Dual-connected topologies. *Int. J. Mech. Sci.* **172**, 105423 (2020)
213. Tian, W., Zhao, T., Yang, Z.: Supersonic meta-plate with tunable-stiffness nonlinear oscillators for nonlinear flutter suppression. *Int. J. Mech. Sci.* **229**, 107533 (2022)
214. Sheng, P., Fang, X., Yu, D., Wen, J.: Nonlinear metamaterial enabled aeroelastic vibration reduction of a supersonic cantilever wing plate. *Appl. Math. Mech.* **34**, 15–25 (2024)
215. Sheng, P., Fang, X., Yu, D., Wen, J.: Mitigating aeroelastic vibration of strongly nonlinear metamaterial supersonic wings under high temperature. *Nonlinear Dyn.* (accepted) (2024)
216. Hu, B., Fang, X., Wen, J., Yu, D.: Effectively reduce transient vibration of 2D wing with bi-stable metamaterial. *Int. J. Mech. Sci.* **272**, 109172 (2024)
217. Fang, X., Wen, J., Cheng, L., Yu, D., Zhang, H., Gumbsch, P.: Programmable gear-based mechanical metamaterials. *Nature Mater.* **21**(8), 869–876 (2022)
218. Zhang, X., Zangeneh-Nejad, F., Chen, Z., Lu, M., Christensen, J.: A second wave of topological phenomena in photonics and acoustics. *Nature* **618**(7966), 687–697 (2023)
219. Chen, Y., Kadic, M., Wegener, M.: Roton-like acoustical dispersion relations in 3D metamaterials. *Nat. Commun.* **12**(1), 3278 (2021)
220. Sepehri, S., Mashhadi, M.M., Fakhrabadi, M.M.S.: Nonlinear nonlocal phononic crystals with roton-like behavior. *Nonlinear Dyn.* **111**(9), 8591–8610 (2023)
221. Duan, Z., Cui, J., Chen, L., Yang, T.: Nonlinear mechanical roton. *J. Appl. Mech.* (2023). <https://doi.org/10.1115/1.4056583>
222. Freundlich, J., Sado, D.: Dynamics of a mechanical system with a spherical pendulum subjected to fractional damping: analytical analysis. *Nonlinear Dyn.* **111**(9), 7961–7973 (2023)
223. Sepehri, S., Mashhadi, M.M., Fakhrabadi, M.M.S.: Wave propagation in fractionally damped nonlinear phononic crystals. *Nonlinear Dyn.* **110**(2), 1683–1708 (2022)
224. Chen, Z., Zhou, W., Lim, C.W.: Active control for acoustic wave propagation in nonlinear diatomic acoustic metamaterials. *Int. J. Non-Linear Mech.* **125**, 103535 (2020)
225. Liu, Z., Shan, S., Cheng, L.: Meta-structure enhanced second harmonic S0 waves for material microstructural changes monitoring. *Ultrasonics* **139**, 107295 (2024)
226. Shan, S., Liu, Z., Zhang, C., Cheng, L., Pan, Y.: A metamaterial-assisted coda wave interferometry method with nonlinear guided waves for local incipient damage monitoring in complex structures. *Smart Mater. Struct.* **33**(3), 035017 (2024)
227. Liu, Z., Shan, S., Cheng, L.: Nonlinear-Lamb-wave-based plastic damage detection assisted by topologically designed metamaterial filters. *Struct. Health Monit.* **22**(3), 1828–1843 (2023)
228. Shan, S., Wen, F., Cheng, L.: Purified nonlinear guided waves through a metamaterial filter for inspection of material microstructural changes. *Smart Mater. Struct.* **30**(9), 095017 (2021)
229. Liu, Z., Shan, S., Dong, H., Cheng, L.: Topologically customized and surface-mounted meta-devices for Lamb wave manipulation. *Smart Mater. Struct.* **31**(6), 065001 (2022)

Publisher's Note Springer Nature remains neutral with regard to jurisdictional claims in published maps and institutional affiliations.